Table 2. Numbers of Podocytes and FSP1$^+$ Podocytes in Renal Biopsy Specimens

Nephropathy	No. of Glomeruli	Podocytes (/glomerular profile)	FSP1$^+$ Podocytes (/glomerular profile)
Diabetic nephropathy			
Grade 1	102	9 (8, 12)*†	1 (0, 2)‡
Grade 2	212	10 (7, 12)†§	2 (1, 4)‖
Grade 3	96	8 (6, 10)†	3 (2, 5)¶
Grade 4	95	6 (4, 8)#	3 (1, 5)¶
Grade 5	57	1 (0, 3)	0 (0, 1)
Minimal change disease	207	9 (7, 11)	0 (0, 1)
Tumor nephrectomy	290	9 (6, 11)	0 (0, 1)

Note: Results expressed as median (first quartile, third quartile).

Abbreviation: FSP1$^+$, fibroblast-specific protein 1 positive.

*$P = 0.02$ versus grade 3.

†$P < 0.001$ versus grades 4 and 5.

‡$P < 0.001$ versus minimal change disease and tumor nephrectomy.

§$P = 0.004$ versus grade 3.

‖$P = 0.007$ versus grade 1.

¶$P < 0.001$ versus grades 1, 2, and 5.

#$P < 0.001$ versus grade 5.

(Fig S2). Finally, we found that ILK colocalized with FSP1 in podocytes from patients with diabetic nephropathy (Fig S3).

Induction of EMT Markers In Vitro

Numerous studies have shown that TGF-β1 is a master regulator governing the induction of EMT, and glomerular TGF-β1 expression is upregulated in diabetic nephropathy.[44,45] We therefore tested whether TGF-β1 stimulates the expression of mesenchymal markers in cultured podocytes. As shown in Fig S4, TGF-β1 induced a more than 6-fold increase in expression of Snail1 mRNA and 3.5-fold increase in that of lysyl oxidase mRNA. Fibronectin and collagen type 1, which are 2 standard mesenchymal markers, were also induced by TGF-β1.

DISCUSSION

Podocytes are specialized visceral epithelial cells that attach to the GBM through $\alpha 3\beta 1$ integrin and dystroglycan.[46] Because the likelihood of detachment is unrelated to the degree of proteinuria in other renal diseases,[47] and in our study, the number of FSP1$^+$ podocytes in patients with MCD is very low, the association of FSP1 expression with detachment probably is indicative of some additional pathophysiological phenomena.

Podocytes detaching from glomeruli are either apoptotic or can be retrieved from urine as viable cells.[13] In diabetes, podocyte detachment is associated with degree of proteinuria, and both detachment and proteinuria can be attenuated by administration of an angiotensin-converting enzyme inhibitor.[12] Apoptosis previously was suggested to be the mechanism underlying podocyte detachment in diabetes, perhaps due to overexpression of TGF-β, alteration of the matrix surrounding the GBM, overexpression of angiotensin II induced by intraglomerular hypertension, high glucose level, proteinuria leading to a decrease in glomerular nephrin, dysfunction of the slit-pore membrane, and/or downregulation of $\alpha 3\beta 1$ integrins.[10,15,16] Because most detached podocytes in our study were not apoptotic, we propose a different mechanism for detachment.

Podocytes rarely express FSP1 in normal glomeruli. The observed upregulation of FSP1 expression in podocytes from patients with diabetes raises the possibility that its expression is linked to podocyte detachment and subsequent glomerular pathological states. In transplantation relapse, primary focal segmental glomerulosclerosis, and idiopathic collapsing glomerulopathy, EMT-like changes are observed in podocytes.[48,49] Because FSP1 is an important regulator of intracellular calcium and actin dynamics in EMT-producing fibroblasts,[21,31] we hypothesize that outside-to-inside signaling induces EMT-like changes and detachment of live podocytes. The presence of FSP1 in a substantial percentage of urinary podocytes in MCD suggests that the same mechanism of podocyte loss may be present in this disease, albeit at a much lower level of activity.

Although there are several regulators of EMT, Snail1 is the most powerful positive regulator of EMT. Snail1 is a zinc-finger transcription factor that binds directly to E-boxes in the promoter regions of E-cadherin, claudin, and occuludin, thereby repressing their expression. It is likely that Snail1 transcription has a critical role in the first steps of EMT by repressing genes encoding adherens and tight junction adhesion molecules. That Snail1 expression is enhanced in diabetic

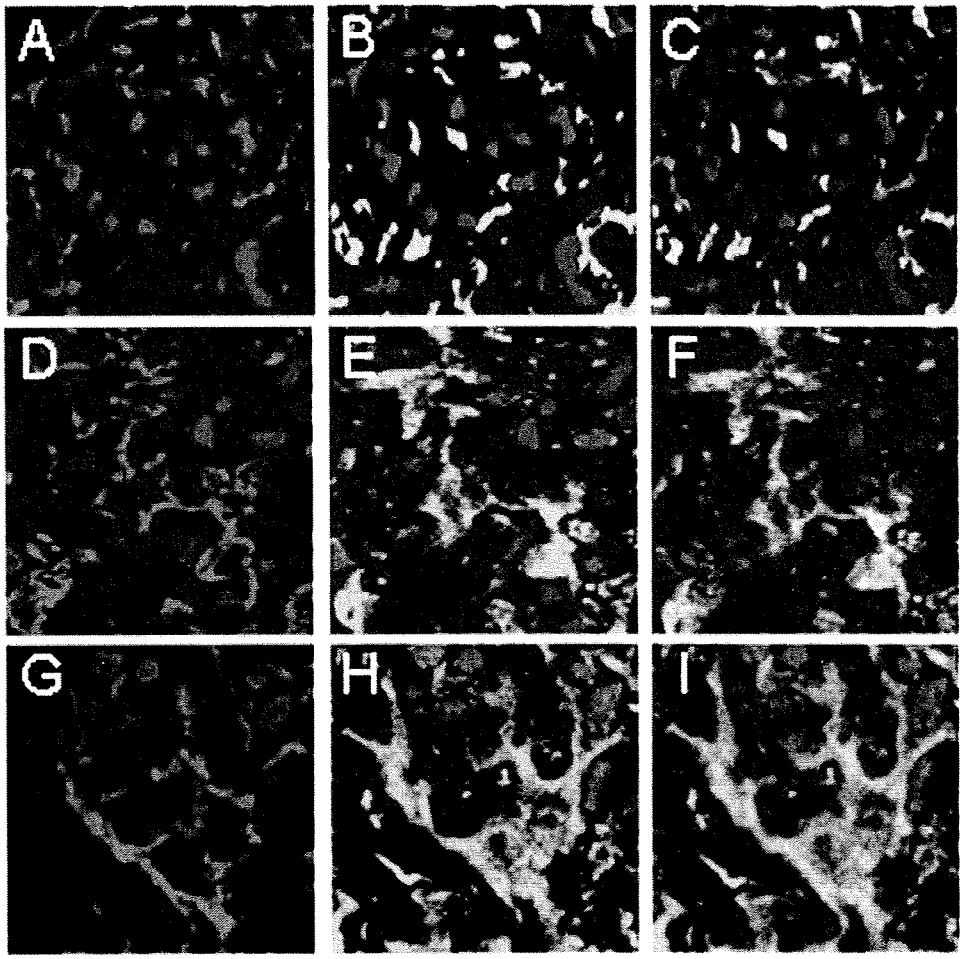

Figure 6. Expression of epithelial-mesenchymal transition markers in renal biopsy specimens from patients with diabetic nephropathy. (A-C) Zona occludens 1 (ZO-1) and fibroblast-specific protein 1 (FSP1) staining in grade 4 diabetic nephropathy. (A) ZO-1 serves as a podocyte marker (red staining). (B) Cells expressing FSP1 (green staining) are clearly present within diabetic glomeruli. (C) Merged images show no colocalization of ZO-1 and FSP1 at advanced stages of diabetic nephropathy. (D-I) Podocyte marker and Snail1 expression in grade 2 diabetic nephropathy. (D, G) Synaptopodin and glomerular epithelial protein 1 (GLEPP1) serve as markers of podocytes (red staining), respectively. (E,H) Cells expressing Snail1 (green staining) are clearly present within diabetic glomeruli. (F, I) Merged images show colocalization of podocyte markers and Snail1, confirming that some podocytes in diabetic glomeruli express Snail1. Nuclei were stained with 4'6-diamidine-2'-phenylindole dihydrochloride (blue). (Original magnification ×400.)

podocytes is consistent with our hypothesis that podocytes undergoing EMT-like change detach from the GBM. Another signaling pathway leading to EMT is through ILK. $\alpha 3\beta 1$ integrins in podocytes are associated with ILK at focal attachment points, and altered expression of $\alpha 3\beta 1$ integrins in the diabetic milieu could activate ILK.[50,51] ILK is expressed by mesangial cells and podocytes in normal glomeruli and upregulated in diabetic glomeruli.[50] High glucose and angiotensin II levels increase ILK expression in cultured podocytes.[51] Activation of ILK in transitioning epithelia induces translocation of β-catenin/lymphoid enhancer-binding factor 1 (LEF-1) complexes into the nucleus, where they reduce E-cadherin expression by engaging the EMT transcriptome.[52] In podocytes, this translocation also represses the slit membrane by reducing expression of P-cadherin and CD2AP.[53] Our observation of the colocalization of FSP1 and ILK in podocytes also supports our hypothesis.

We suggest that TGF-β1 is the effector most likely to elicit EMT in diabetic neuropathy. TGF-β1 is upregulated in glomeruli of patients

with diabetes[44,45] and is the master regulator governing induction of EMT.[19] Moreover, we found that TGF-β1 stimulated expression of Snail1 and lysyl oxidase in cultured podocytes. Because both these effectors stimulate cellular motility,[43,54] we suggest they also may be associated with podocyte detachment.

In summary, our new finding of FSP1 in human podocytes from diabetic glomeruli is consistent with the notion that EMT-like changes may explain podocyte detachment in diabetic nephropathy. The number of $FSP1^+$ podocytes in renal biopsy specimens and urine sediment may be predictive of renal disease progression. Elucidation of the mechanisms regulating FSP1 expression in podocytes should shed new light on processes governing the pathogenesis of human diabetic nephropathy.

ACKNOWLEDGEMENTS

We thank Dr Peter Mundel, Miami Institute of Renal Medicine, University of Miami, for providing an immortalized podocyte cell line and Ms Hiromi Ohura, Ms Fumika Kunda, and Ms Miyako Sakaida for their excellent technical assistance. Part of this study was presented in abstract form at the 39th Annual Meeting of the American Society of Nephrology, November 14-19, 2006, San Diego, CA.

Support: This work was supported in part by research Grant 19590960 to Dr Iwano from the Ministry of Education and Science of Japan. Dr Neilson is supported by National Institutes of Health Grant DK-46282.

Financial Disclosure: None.

SUPPLEMENTARY MATERIAL

Figure S1. Representative immunohistochemical evaluation of a renal biopsy specimen from a patient with minimal change disease.

Figure S2. Expression of epithelial-mesenchymal transition markers in a renal biopsy specimen from a patient with minimal change disease.

Figure S3. FSP1 and ILK expression in minimal change disease and diabetic nephropathy.

Figure S4. Induction of mesenchymal markers in cultured podocytes after stimulation with TGF-β1.

Note: The supplementary material accompanying this article (doi:10.1053/j.ajkd.2009.05.009) is available at www.ajkd.org.

REFERENCES

1. Osterby R, Gall MA, Schmitz A, Nielsen FS, Nyberg G, Parving HH: Glomerular structure and function in proteinuric type 2 (non-insulin-dependent) diabetic patients. Diabetologia 36:1064-1070, 1993

2. White KE, Bilous RW: Type 2 diabetic patients with nephropathy show structural-functional relationships that are similar to type 1 disease. J Am Soc Nephrol 11:1667-1673, 2000

3. Lemley KV: Diabetes and chronic kidney disease: Lessons from the Pima Indians. Pediatr Nephrol 23:1933-1940, 2008

4. Abouna GM, Al-Adnani MS, Kremer GD, Kumar SA, Daddah SK, Kusma G: Reversal of diabetic nephropathy in human cadaveric kidneys after transplantation into non-diabetic recipients. Lancet 2:1274-1276, 1983

5. Fioretto P, Steffes MW, Sutherland DE, Goetz FC, Mauer M: Reversal of lesions of diabetic nephropathy after pancreas transplantation. N Engl J Med 339:69-75, 1998

6. Pagtalunan ME, Miller PL, Jumping-Eagle S, et al: Podocyte loss and progressive glomerular injury in type II diabetes. J Clin Invest 99:342-348, 1997

7. Meyer TW, Bennett PH, Nelson RG: Podocyte number predicts long-term urinary albumin excretion in Pima Indians with type II diabetes and microalbuminuria. Diabetologia 42:1341-1344, 1999

8. Dalla Vestra M, Masiero A, Roiter AM, Saller A, Crepaldi G, Fioretto P: Is podocyte injury relevant in diabetic nephropathy? Studies in patients with type 2 diabetes. Diabetes 52:1031-1035, 2003

9. White KE, Bilous RW: Structural alterations to the podocyte are related to proteinuria in type 2 diabetic patients. Nephrol Dial Transplant 19:1437-1440, 2004

10. Wolf G, Chen S, Ziyadeh FN: From the periphery of the glomerular capillary wall toward the center of disease: Podocyte injury comes of age in diabetic nephropathy. Diabetes 54:1626-1634, 2005

11. Lemley KV, Lafayette RA, Safari M, et al: Podocytopenia and disease severity in IgA nephropathy. Kidney Int 61:1475-1485, 2002

12. Nakamura T, Ushiyama C, Suzuki S, et al: Urinary excretion of podocytes in patients with diabetic nephropathy. Nephrol Dial Transplant 15:1379-1383, 2000

13. Vogelmann SU, Nelson WJ, Myers BD, Lemely KV: Urinary excretion of viable podocytes in health and renal disease. Am J Physiol Renal Physiol 285:F40-F48, 2003

14. Chen HC, Chen CA, Guh JY, Chang JM, Shin SJ, Lai YH: Altering expression of alpha3beta1 integrin on podocytes of human and rats with diabetes. Life Sci 67:2345-2353, 2000

15. Schiffer M, Bitzer M, Roberts IS, et al: Apoptosis in podocytes induced by TGF-beta and Smad7. J Clin Invest 108:807-816, 2001

16. Ding G, Reddy K, Kapasi AA, et al: Angiotensin II induces apoptosis in rat glomerular epithelial cells. Am J Physiol Renal Physiol 283:F173-F180, 2002

17. Kumar D, Robertson S, Burns KD: Evidence of apoptosis in human diabetic kidney. Mol Cell Biochem 259:67-70, 2004

18. Verzola D, Gandolfo MT, Ferrario F, et al: Apoptosis in the kidneys of patients with type II diabetic nephropathy. Kidney Int 72:1262-1272, 2007

19. Li Y, Kang YS, Dai C, Kiss LP, Wen X, Liu Y: Epithelial-to-mesenchymal transition is a potential pathway leading to podocyte dysfunction and proteinuria. Am J Pathol 172:299-308, 2008

20. Strutz F, Okada H, Lo CW, et al: Identification and characterization of a fibroblast marker: FSP1. J Cell Biol 130:393-405, 1995

21. Iwano M, Plieth D, Danoff TM, Xue C, Okada H, Neilson EG: Evidence that fibroblasts derive from epithelium during tissue fibrosis. J Clin Invest 110:341-350, 2002

22. Barraclough R: Calcium-binding protein S100A4 in health and disease. Biochim Biophys Acta 1448:190-199, 1998

23. Donato R: S100: A multigenic family of calcium-modulated proteins of the EF-hand type with intracellular and extracellular functional roles. Int J Biochem Cell Biol 33:637-668, 2001

24. Donato R: Intracellular and extracellular roles of S100 proteins. Microsc Res Tech 60:540-551, 2003

25. Okada H, Danoff TM, Kalluri R, Neilson EG: Early role of Fsp1 in epithelial-mesenchymal transformation. Am J Physiol Renal Physiol 273:F563-F574, 1997

26. Okada H, Ban S, Nagao S, Takahashi H, Suzuki H, Neilson EG: Progressive renal fibrosis in murine polycystic kidney disease: An immunohistochemical observation. Kidney Int 58:587-597, 2000

27. Iwano M, Fischer A, Okada H, et al: Conditional abatement of tissue fibrosis using nucleoside analogs to selectively corrupt DNA replication in transgenic fibroblasts. Mol Ther 3:149-159, 2001

28. Strutz F, Neilson EG: New insights into mechanisms of fibrosis in immune renal injury. Springer Semin Immunopathol 24:459-476, 2003

29. Iwano M, Neilson EG: Mechanisms of tubulointerstitial fibrosis. Curr Opin Nephrol Hypertens 13:279-284, 2004

30. Nishitani Y, Iwano M, Yamaguchi Y, et al: Fibroblast-specific protein 1 is a specific prognostic marker for renal survival in patients with IgAN. Kidney Int 68:1078-1085, 2005

31. Kalluri R, Neilson EG: Epithelial-mesenchymal transition and its implications for fibrosis. J Clin Invest 112:1776-1784, 2003

32. Imai E, Horio M, Iseki K, et al: Prevalence of chronic kidney disease (CKD) in the Japanese general population predicted by the MDRD equation modified by a Japanese coefficient. Clin Exp Nephrol 11:156-163, 2007

33. Cockcroft DW, Gault MH: Prediction of creatinine clearance from serum creatinine. Nephron 16:31-41, 1976

34. Hara M, Yamamoto T, Yanagihara T, et al: Urinary excretion of podocalyxin indicates glomerular epithelial cell injuries in glomerulonephritis. Nephron 69:397-403, 1995

35. Hara M, Yanagihara T, Takada T, et al: Urinary excretion of podocytes reflects disease activity in children with glomerulonephritis. Am J Nephrol 18:35-41, 1998

36. Hara M, Yanagihara T, Kihara I: Cumulative excretion of urinary podocytes reflects disease progression in IgA nephropathy and Schönlein-Henoch purpura nephritis. Clin J Am Soc Nephrol 2:231-238, 2007

37. Suzuki D, Miyazaki M, Naka R, et al: In situ hybridization of interleukin 6 in diabetic nephropathy. Diabetes 44:1233-1238, 1995

38. Yoshimoto S, Nakatani K, Iwano M, et al: Elevated levels of fractalkine expression and accumulation of $CD16^+$ monocytes in glomeruli of active lupus nephritis. Am J Kidney Dis 50:47-58, 2007

39. Garrett SC, Varney KM, Weber DJ, Bresnick AR: S100A4, a mediator of metastasis. J Biol Chemi 281:677-680, 2006

40. Riccioni R, Calzolari A, Biffoni M, et al: Podocalyxin is expressed in normal and leukemic monocytes. Blood Cells Mol Dis 37:218-225, 2006

41. Skoberne A, Konieczny A, Schiffer M: Glomerular epithelial cells in the urine: What has to be done to make them worthwhile? Am J Physiol Renal Physiol 296:230-241, 2009

42. Horvat R, Hovorka A, Dekan G, Poczewski H, Kerjaschki D: Endothelial cell membranes contain podocalyxin—The major sialoprotein of visceral glomerular epithelial cells. J Cell Biol 102:484-491, 1986

43. Rowe RG, Li XY, Hu Y, et al: Mesenchymal cells reactivate Snail1 expression to drive three-dimensional invasion programs. J Cell Biol 184:399-408, 2009

44. Iwano M, Kubo A, Nishino T, et al: Quantification of glomerular TGF-beta 1 mRNA in patients with diabetes mellitus. Kidney Int 49:1120-1126, 1996

45. Yamamoto T, Nakamura T, Noble NA, Ruoslahti E, Border WA: Expression of transforming growth factor beta is elevated in human and experimental diabetic nephropathy. Proc Natl Acad Sci U S A 90:1814-1818, 1993

46. Kretzler M: Regulation of adhesive interaction between podocytes and glomerular basement membrane. Microsc Res Tech 57:247-253, 2002

47. Lahdenkari AT, Lounatmaa K, Patrakka J, et al: Podocytes are firmly attached to glomerular basement membrane in kidneys with heavy proteinuria. J Am Soc Nephrol 15:2611-2618, 2004

48. Bariety J, Nochy D, Mandet C, Jacquot C, Glotz D, Meyrier A: Podocytes undergo phenotypic changes and express macrophagic-associated markers in idiopathic collapsing glomerulopathy. Kidney Int 53:918-925, 1998

49. Bariety J, Bruneval P, Hill G, Irinopoulou T, Mandet C, Meyrier A: Posttransplantation relapse of FSGS is characterized by glomerular epithelial cell transdifferentiation. J Am Soc Nephrol 12:261-274, 2001

50. Guo L, Sanders PW, Woods A, Wu C: The distribution and regulation of integrin-linked kinase in normal and diabetic kidneys. Am J Pathol 159:1735-1742, 2001

51. Han SY, Kang YS, Jee YH, et al: High glucose and angiotensin II increase beta1 integrin and integrin-linked kinase synthesis in cultured mouse podocytes. Cell Tissue Res 323:321-332, 2006

52. Novak A, Hsu SC, Leung-Hagesteijn C, et al: Cell adhesion and the integrin-linked kinase regulate the LEF-1 and beta-catenin signaling pathways. Proc Natl Acad Sci U S A 95:4374-4379, 1998

53. Teixeira Vde P, Blattner SM, Li M, et al: Functional consequences of integrin-linked kinase activation in podocyte damage. Kidney Int 67:514-523, 2005

54. Higgins DF, Kimura K, Bernhardt WM, et al: Hypoxia promotes fibrogenesis in vivo via HIF-1 stimulation of epithelial-to-mesenchymal transition. J Clin Invest 117:3810-3820, 2007

Guanylyl Cyclase-A Inhibits Angiotensin II Type 2 Receptor-Mediated Pro-Hypertrophic Signaling in the Heart

Yuhao Li, Yoshihiko Saito, Koichiro Kuwahara, Xianglu Rong, Ichiro Kishimoto, Masaki Harada, Yuichiro Adachi, Michio Nakanishi, Hideyuki Kinoshita, Masatsugu Horiuchi, Michael Murray, and Kazuwa Nakao

Department of Medicine and Clinical Science (Y.L., K.K., X.R., M.H., Y.A., M.N., H.K., K.N.), Kyoto University Graduate School of Medicine, Kyoto 606-8507, Japan; First Department of Internal Medicine (Y.S.), Nara Medical University, Nara 634, Japan; National Cardiovascular Center Research Institute (I.K.), Osaka 565-8565, Japan; Department of Molecular Cardiovascular Biology and Pharmacology (M.H.), Ehime University Graduate School of Medicine, Ehime 791-0295, Japan; and Faculty of Pharmacy (M.M.), The University of Sydney, Sydney, New South Wales 2006, Australia

Angiotensin II plays a key role in the development of cardiac hypertrophy. The contribution of the angiotensin II type 1 receptor (AT1) in angiotensin II-induced cardiac hypertrophy is well established, but the role of AT2 signaling remains controversial. Previously, we have shown that natriuretic peptide receptor/guanylyl cyclase-A (GCA) signaling protects the heart from hypertrophy at least in part by inhibiting AT1-mediated pro-hypertrophic signaling. Here, we investigated the role of AT2 in cardiac hypertrophy observed in mice lacking GCA. Real-time RT-PCR and immunoblotting approaches indicated that the cardiac AT2 gene was overexpressed in GCA-deficient mice. Mice lacking AT2 alone did not exhibit an abnormal cardiac phenotype. In contrast, GCA-deficiency-induced increases in heart to body weight ratio, cardiomyocyte cross-sectional area, and collagen accumulation as evidenced by van Gieson staining were attenuated when AT2 was absent. Furthermore, the up-regulated cardiac expression of hypertrophy-related genes in GCA-null animals was also suppressed. Pharmacological blockade of AT2 with PD123319 similarly attenuated cardiac hypertrophy in GCA-deficient mice. In addition, whereas the AT1 antagonist olmesartan attenuated cardiac hypertrophy in GCA-deficient mice, this treatment was without effect on cardiac hypertrophy in GCA/AT2-double null mice, notwithstanding its potent antihypertensive effect in these animals. These results suggest that the interplay of AT2 and AT1 may be important in the development of cardiac hypertrophy. Collectively, our findings support the assertion that GCA inhibits AT2-mediated pro-hypertrophic signaling in heart and offer new insights into endogenous cardioprotective mechanisms during disease pathogenesis. (***Endocrinology*** **150: 3759–3765, 2009)**

Cardiac hypertrophy is an independent risk factor for cardiac morbidity and mortality. Left ventricular hypertrophy is a major, independent predictor of cardiovascular events, particularly in hypertension, in which it dramatically increases the risk of stroke, coronary heart disease, and heart failure (1). Therefore, elucidation of the underlying mechanism leading to cardiac hypertrophy may have significant implications for the development of therapeutic strategies.

Atrial natriuretic peptide (ANP) is a cardiac hormone that acts through guanylate cyclase-A (GCA) to lower blood pressure and dilate blood vessels *in vivo* (2) and to inhibit the growth of cardiac myocytes and fibroblasts *in vitro* (3). Brain natriuretic peptide (BNP) also activates GCA and has effects similar to those of ANP, although it also exerts local antifibrotic actions in the ventricle (4). Mice lacking GCA exhibit hypertension, cardiac hypertrophy, and fibrosis and are prone to sudden death, which is consistent with a protective role for natriuretic peptide/GCA-signaling pathways in the cardiovascular system (5–8).

Angiotensin (Ang) II plays a key role in the development of cardiac hypertrophy (9). Although most of the cardiovascular

ISSN Print 0013-7227 ISSN Online 1945-7170
Printed in U.S.A.

doi: 10.1210/en.2008-1353 Received September 18, 2008. Accepted April 6, 2009.
First Published Online April 16, 2009

Abbreviations: ACE, Angiotensin converting enzyme; Agt, angiotensinogen; Ang, angiotensin; ANP, atrial natriuretic peptide; AT1, angiotensin II type 1 receptor; BNP, brain natriuretic peptide; BW, body weight; GCA, guanylyl cyclase-A; HW, heart weight; KO, knockout; LVW, left ventricular weight; NPR, natriuretic peptide receptor; RVW, right ventricular weight; SBP, systolic blood pressure; WT, wild type.

effects of Ang II are mediated via the Ang II type 1 receptor (AT1) (10), the alternate major Ang II receptor subtype, AT2, may also be important because its expression is up-regulated in cardiovascular pathologies, including cardiac hypertrophy (11, 12) and heart failure (13). Although the roles of AT2 in cardiac remodeling remain controversial, accumulating lines of evidence appear to support the view that AT2 can promote cardiac growth in pathological situations. Indeed, at least in some tissues, AT1 and AT2 share common signaling pathways that stimulate cell and tissue proliferation (14–18).

We have demonstrated previously that genetic or pharmacological blockade of AT1a signaling attenuates cardiac hypertrophy and fibrosis in GCA-deficient mice (6, 7), suggesting that GCA inhibits AT1a-mediated pathological signaling in the heart. Importantly, however, the cardiac hypertrophy and fibrosis in GCA-deficient mice was not completely abolished in animals lacking both GCA and AT1a (6). Similarly, AT1 blockade by olmesartan (CS-866) in GCA-null mice only partially reversed the increase in cardiac hypertrophy and fibrosis, suggesting the involvement of AT1-independent signaling in cardiac remodeling observed in GCA-deficient mice. In the present study, we investigated the role played by AT2 in cardiac hypertrophy induced by GCA deficiency using further genetic and pharmacological manipulation in mice. The findings of this study are consistent with a pro-hypertrophic effect of AT2 signaling in heart.

Materials and Methods

Animals and treatments

All experimental procedures were performed according to Kyoto University standards for animal care.

Experiment 1

Male homozygous GCA-deficient [$GCA^{-/-}/AT2^{+/y}$, GCA knockout (KO)] and wild-type (WT, $GCA^{+/+}/AT2^{+/y}$) mice used in this experiment (n = 7 each group) were generated by methods described previously (5). The genetic backgrounds of the mice were C57BL/6. Animals at 16–17 wk of age were killed for initial gene analysis.

Experiment 2

The genetic backgrounds of the AT2-deficient ($GCA^{+/-}/AT2^{-/y}$, AT2 KO) mice were FVB/N. Male homozygous AT2 KO, GCA KO, $GCA^{-/-}/AT2^{-/y}$ (double KO), and WT mice used in this experiment (n = 7–9 each group) were generated from the heterozygotes after crossing female AT2 KO and male GCA KO mice. Systolic blood pressure (SBP) was measured at 11, 14, and 16 wk of age using a noninvasive computerized tail-cuff method (BP98A; Softron Co., Ltd., Tokyo, Japan) (6–8). Animals at 16–17 wk of age were killed for further examination.

Experiment 3

WT and GCA KO mice were used in this experiment (n = 5 each group). The AT2 antagonist PD123319 (30 mg/kg · d; Sigma, Osaka, Japan) was dissolved in saline and administered daily by ip injection for 4 wk, in mice at 12–13 wk of age. The corresponding control animals were treated with saline only. SBP was measured before and 2 and 3 wk after treatment with the antagonist or saline using a tail-cuff method (MK-2000ST; Muromachi Kikai Co. Ltd., Tokyo, Japan). Animals were killed for further examination after 4 wk treatment.

Experiment 4

All four genotypes were used in this experiment (n = 7–9 each group). The AT1 antagonist olmesartan (a gift from Daiichi-Sankyo Co. Ltd., Tokyo, Japan) was suspended in 5% gum arabic and administered by oral gavage at a dose of 10 mg/kg once a day for 4 wk in mice at 12–13 wk of age; control animals received vehicle alone. SBP was measured 3 wk after treatment with the antagonist or vehicle using a tail-cuff method (BP98A; Softron). Animals were killed for further examination after 4 wk treatment.

Determination of heart weight (HW) and right and left ventricular weights (RVW and LVW)

Animals were euthanized, hearts were removed and weighed, and then the right and left ventricles were weighed separately. The ratios of these weights to the total body weight (BW) (HW/BW, RVW/BW, and LVW/BW) were calculated as indexes of cardiac hypertrophy.

Measurement of cardiomyocyte cross-sectional area and histological assessment of cardiac fibrosis

A segment of the excised left ventricle from each animal was fixed in 10% neutral formalin over several days and then dehydrated with graded concentrations of alcohol before embedding in paraffin. Paraffin slices from each heart were stained with hematoxylin-eosin. Morphometry of each section was performed to determine the myocyte cross-sectional area as described previously (19). The cross-sectional area of cardiomyocytes in sections that had been cut transversely was measured using a KS400 Imaging System (Carl Zeiss Vision, Eching, Germany); cardiomyocytes possessed an intact cellular membrane, and the nucleus was visible. The outer borders of the cardiomyocytes were traced at × 400 magnification, and the cardiomyocyte areas were calculated. One hundred cells per heart were counted, and the mean value was used in subsequent analyses.

To determine the extent of collagen fiber accumulation, paraffin slices from each heart were subjected to van Gieson staining. Forty fields from three individual sections were selected at random, and the van Gieson-stained areas were measured in relation to the total left ventricular area using image analysis software and a Zeiss KS400 system (6, 7).

Analysis of mRNA

Total RNA was prepared from individual left ventricles of mouse hearts using TRIzol (Life Technologies Inc., Rockville, MD). mRNAs were quantified by real-time RT-PCR using the TaqMan system (ABI PRISM 7700 Sequence Detector; Applied Biosystems, Foster City, CA) (6). The primers and probes of the genes examined were as follows: ANP sense 5′-GCCATATTGGAGCAAATCCT-3′, antisense 5′-GCAGGTTCTTGAAATCCATCA-3′, and oligonucleotide probe, 5′-TGTACAGTGCGGTGTCCAACACAGAT-3′; BNP sense 5′-CCAGTCTCCAGAGCAATTCAA-3′, antisense 5′-GCCATTTCCTCCGACTTTT-3′, and oligonucleotide probe 5′-TGCAGAAGCTGCTGGAGCTGATAAGA-3′; collagen I sense 5′-GTCCCAACCCCCAAAGAC-3′, antisense 5′-CATCTTCTGAGTTTGGTGATACGT-3′, and oligonucleotide probe 5′-CACGGCTGTGTGCGATGACG-3′; collagen III sense 5′-TGGTTTCTTCTCACCCTTCTTC-3′, antisense 5′-TGCATCCCAATTCATCTACGT-3′, and oligonucleotide probe 5′-TCCCACTCTTATTTTGGCACAGCAGTC-3′; angiotensinogen (Agt) sense 5′-CATTGGTGACACCAACCCC-3′, antisense 5′-GCTGTTCCTCCTCTCCTGCT-3′, and oligonucleotide probe 5′-AGGTTCTCAATAGCATCCTCCTCGAACTC-3′; angiotensin converting enzyme (ACE) sense 5′-CGGAATGAAACCCATTTTGA-3′, antisense 5′-GCACAAAGCTCACGAAGTACC-3′, and oligonucleotide probe 5′-CACATCCCAAACGTGACACCGTACAT-3′; AT1a sense 5′-GTTTGCGCTTTTCATTACGAGT-3′, antisense 5′-TCTTGGTTAGGCCCAGTCCT-3′, and oligonucleotide probe 5′-CCGGAATTCAACGCTCCCCA-3′; AT2 sense 5′-CCACCA GCAGAAACATTACC-3′, antisense 5′-GGACTCATTGGTGCCAGTT-3′, and oligonucleotide probe 5′-CAGCCGTCCTTTTGATAATCTCAACG-3′; and TGF-β1 sense 5′-GACGTCACTGGAGTTGTACGG-3′, antisense 5′-GCTGA-

ATCGAAAGCCCTGT-3′, and oligonucleotide probe 5′-AGCGCATC-GAAGCCATCCG −3′. Glyceraldehyde-3-phosphate dehydrogenase (housekeeping gene) mRNA was also amplified with specific primers and probe (Applied Biosystems).

Immunoblotting

AT2 protein was estimated by Western blotting (20). Total proteins were resolved on 4–12% polyacrylamide gradient gels (Invitrogen, Carlsbad, CA), electrophoretically transferred to polyvinylidene difluoride membranes, blocked [in buffer containing 20 mM Tris (pH 7.5), 150 mM NaCl, 5% BSA, 0.1% Tween 20], and incubated for 18 h at 4 C with AT2 receptor-specific antibody (Santa Cruz Biotechnology, Santa Cruz, CA). Detection was performed with peroxidase-conjugated secondary antibody, using an ECL chemiluminescence kit (Amersham, Buckinghamshire, UK). Immunoblotting with a monoclonal anti-β-actin antibody (Cell Signaling, Beverly, MA) was conducted to ensure equal protein loading.

Statistical analysis

All results are expressed as means ± SEM of values obtained in individual animals. Data were analyzed by single-factor ANOVA. If a significant effect was found, the Fisher's protected least significant difference test was performed to isolate the difference between the groups. Student's *t* test was used to assess the effect of olmesartan treatment on the hypertrophic phenotype in GCA KO mice (see Fig. 6). A value of $P < 0.05$ was considered to be statistically significant.

Results

AT2 deficiency ameliorates cardiac hypertrophy in GCA-deficient mice

We first determined cardiac gene expression of AT2 and AT1a in WT and GCA KO mice using real-time RT-PCR analysis. The results demonstrated an increase in cardiac AT2 mRNA expression in GCA-deficient mice compared with WT controls (Fig. 1A). Western blot analysis confirmed the increase in AT2 expression in GCA-null mouse heart at the protein level (Fig. 1B). In contrast, cardiac AT1a mRNA expression did not differ between WT and GCA null mice (Fig. 1C). There were no differences in the cardiac expression of Agt and ACE between WT and GCA-KO (data not shown).

To evaluate the potential role of AT2 in cardiac hypertrophy induced by GCA deficiency, we generated mice lacking both GCA and AT2 by crossing AT2 KO and GCA KO mice. There was no significant difference in BW among the four genotypes (WT, 34.1 ± 1.1 g; AT2 KO, 34.3 ± 1.1 g; GCA KO, 35.4 ± 1.1 g; double KO, 34.3 ± 0.7 g). In accord with previous reports (15, 16, 21), single deletion of AT2 did not induce a change in cardiac phenotype (Figs. 2, A–D, and 3, A, B, D, and H). By contrast, deletion of GCA alone increased SBP (Fig. 2A), HW/BW (Fig. 2B), LVW/BW (Fig. 2C), RVW/BW (Fig. 2D), the cross-sectional area of cardiomyocytes (Fig. 3, A and E), and cardiac interstitial van Gieson-staining area (Fig. 3, B and I). Importantly, SBP was not different between GCA KO and double KO mice (Fig. 2A), whereas HW/BW, LVW/BW, and RVW/BW ratios, the cross-sectional area of cardiomyocytes, and left ventricular interstitial fibrosis were all lower in double KO mice compared with GCA KO animals (Figs. 2, B–D, and 3, A, B, F, and J).

We further examined the expression of hypertrophy-related genes. Cardiomyocytes are the major source of ANP and BNP (2), which are two important molecular markers of cardiomyocyte hypertrophy (22). Collagens I and III are the principal collagen genes expressed in heart. Consistent with the changes in cardiac hypertrophy and fibrosis, deletion of AT2 alone did not alter cardiac expression of mRNAs for ANP, BNP, and collagens I and III in mice (Fig. 4, A–D). However, the increased cardiac expression of each of these genes that was observed in mice that lacked GCA was suppressed when AT2 was also deleted (Fig. 4, A–D).

To investigate the underlying mechanism, we further examined cardiac expression of Agt, ACE, AT1a, and TGF-β1 mRNAs. No differences in the expression of Agt, ACE, and AT1a mRNAs were observed between genotypes (Fig. 4, E–G). Single

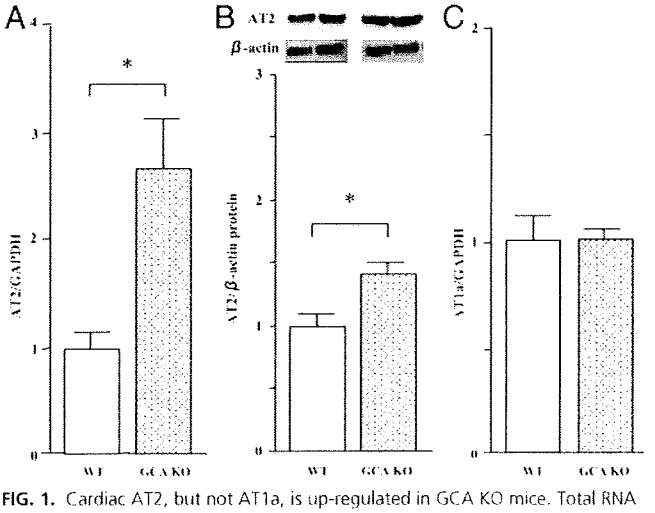

FIG. 1. Cardiac AT2, but not AT1a, is up-regulated in GCA KO mice. Total RNA was extracted from the left ventricular tissues using TRIzol. A and C, AT2 (A) and AT1a (C) mRNAs were determined by real-time RT-PCR, and the results were normalized to GAPDH. B, AT2 protein was detected by Western immunoblot analysis. Values are means ± SEM (n = 7). *, $P < 0.05$.

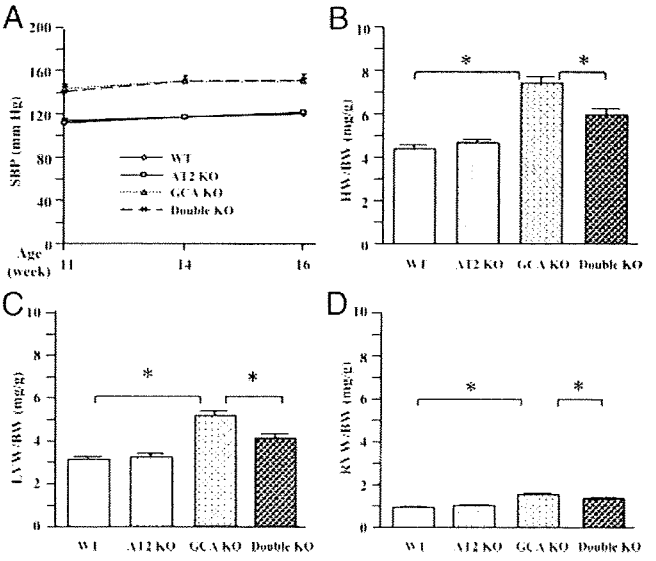

FIG. 2. Targeted deletion of AT2 ameliorated cardiac hypertrophy in GCA-deficient mice. A–D, SBP (A), HW/BW (B), LVW/BW (C), and RVW/BW (D) in WT, AT2 KO, GCA KO, and AT2/GCA double KO mice. Values are means ± SEM (n = 7–9). *, $P < 0.05$.

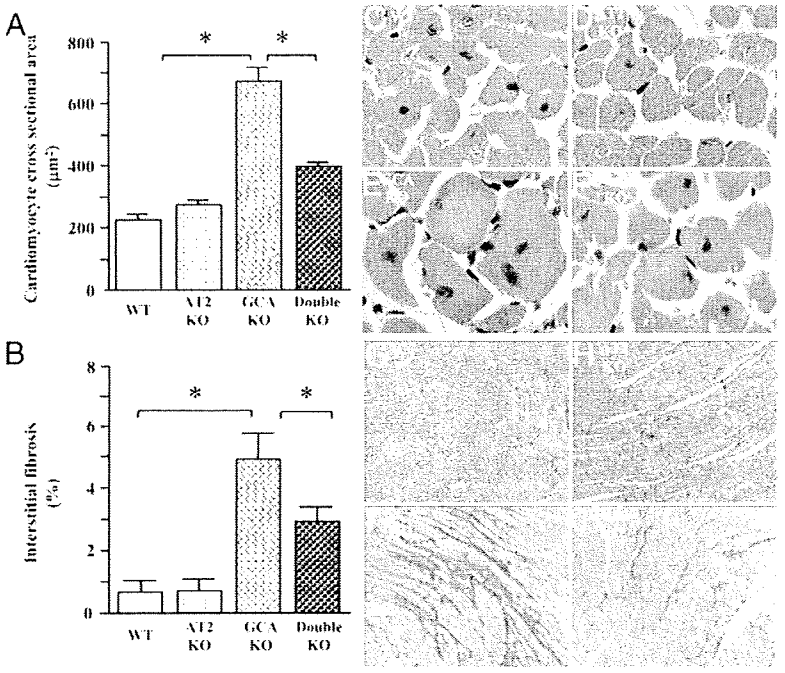

FIG. 3. Deletion of AT2 decreased cardiomyocyte cross-sectional areas and cardiac interstitial fibrosis in GCA-deficient mice. Morphometry of left ventricular myocytes was performed to measure the myocyte cross-sectional area as described previously (19). The van Gieson-stained collagen deposit area and total ventricular area in the left ventricles were analyzed using an image analyzing system. A, Cardiomyocyte cross-sectional areas in the four mouse genotypes under investigation; B, interstitial fibrosis (percent, the van Gieson-stained area to total ventricular area ratio); C–F, representative histological findings of cardiomyocytes in different experimental groups (hematoxylin-eosin staining). Magnification, ×400. G–J, Representative examples of cardiac interstitial fibrosis (*red*; ×200). Values are means ± SEM (n = 7–9). *, $P < 0.05$.

deletion of AT2 did not alter cardiac expression of TGF-β1 (Fig. 4H). However, TGF-β1 gene expression was significantly up-regulated in cardiac tissues from GCA KO mice. Consistent with the observed attenuation of cardiac hypertrophy and fibrosis, TGF-β1 expression in double KO mice was returned to the levels observed in hearts from WT mice.

Pharmacological blockade of AT2 also attenuates cardiac hypertrophy in GCA-deficient mice

To substantiate the role of AT2 in GCA deficiency-induced cardiac hypertrophy, we administered the AT2 antagonist PD123319 to GCA-null mice. Consistent with genetic blockade of AT2, PD123319 treatment for 4 wk did not affect SBP (Fig. 5A) but decreased the ratios of HW/BW and LVW/BW in GCA KO mice (Fig. 5, B and C); RVW/BW ratio was unchanged (Fig. 5D).

Residual cardiac hypertrophy in double KO mice is resistant to an AT1 antagonist

Pharmacological or genetic blockade of AT1 has been shown to attenuate GCA-deficiency-induced cardiac hypertrophy (6). Although cardiac mass in double KO mice was significantly lower than in GCA KO mice, it was still greater than that in WT and AT2 KO mice (Fig. 2, B–D). To test whether the residual hypertrophic effect might be mediated by AT1, we administered the AT1 antagonist olmesartan to WT, AT2 KO, GCA KO, and double KO mice. Olmesartan treatment similarly decreased SBP in all four of the murine genotypes under investigation (Fig. 6A). However, whereas this treatment significantly reduced HW/BW (Fig. 6B) and LVW/BW (Fig. 6C) in GCA KO, it was without effect in double KO mice.

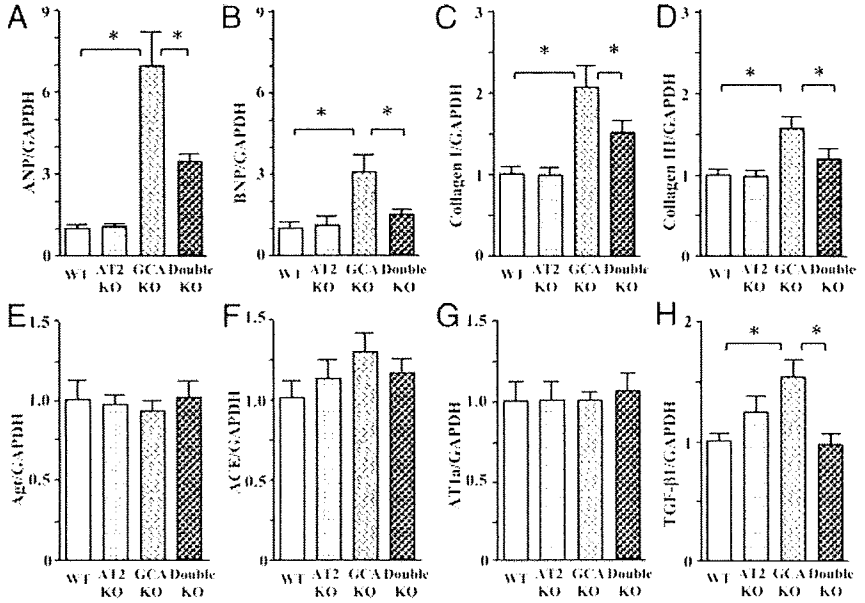

FIG. 4. Cardiac mRNA expression of the ANP (A), BNP (B), collagen I (C), collagen III (D), Agt (E), ACE (F), AT1a (G), and TGF-β1 (H) genes among different mouse genotypes. Total RNA was extracted from the left ventricular tissues using TRIzol. The relative levels of specific mRNAs were determined by real-time RT-PCR. Results were normalized to GAPDH. Values are means ± SEM (n = 7–9). *, $P < 0.05$.

Discussion

The role of AT2-mediated signaling pathways in the development of cardiac hypertrophy remains controversial. Initially, AT2 was reported to exert opposing effects on growth-promoting signaling mediated by AT1 (23). On the other hand, there are several reports that AT2 activates pro-hypertrophic signaling in some animal models (15, 16, 18). Thus, AT2 may have complex effects in the development of cardiovascular hypertrophy (24). It has been reported that the expression of AT2, but not AT1, is directly correlated with left ventricular mass in aortic-banded rats that exhibit cardiac hypertrophy (11, 25). In accord with these reports, the present findings from real-time RT-PCR and immunoblot analyses demonstrated that AT2, but not AT1a, was up-regulated in GCA KO mouse heart. Although deletion of AT2 alone did not induce a change in cardiac phenotype, the increase in cardiac mass reflected by increased ratios

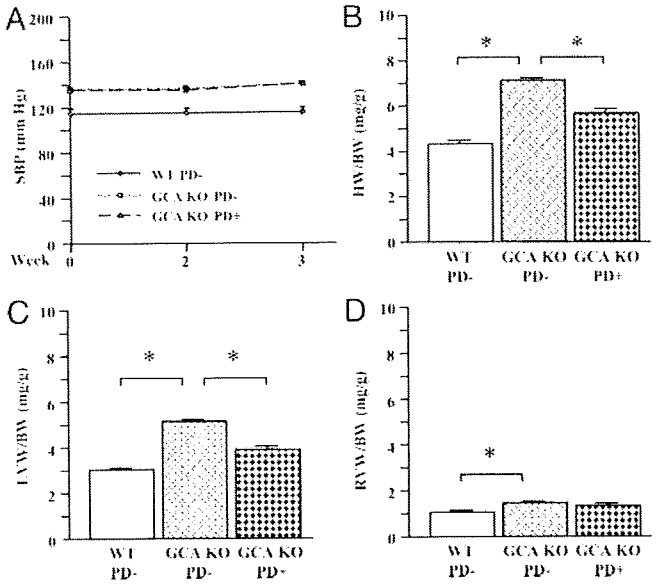

FIG. 5. Pharmacological blockade of AT2 ameliorated cardiac hypertrophy but did not affect hypertension in GCA-deficient mice. The AT2 antagonist PD123319 (30 mg/kg) was injected (ip) daily for 4 wk. The corresponding control animals were treated with saline alone. A–D, SBP (A), HW/BW (B), LVW/BW (C), and RVW/BW (D) in saline-treated (PD−) or PD123319-treated (PD+) mice. Values are means ± SEM (n = 5 each group). *, $P < 0.05$.

of cardiac weights to body weight, cardiomyocyte cross-sectional area, and collagen accumulation and overexpression of hypertrophic genes ANP, BNP, and collagens I and III in GCA-deficient hearts were all suppressed by AT2 deletion. Similarly, the cardiac hypertrophy in GCA-deficient mice was also attenuated by pharmacological blockade with PD123319. These results clearly indicate that AT2-dependent pro-hypertrophic signaling is dependent on GCA deficiency. Thus, similar to the situation with AT1a (6), AT2-mediated pro-hypertrophic signaling in the heart is inhibited by GCA.

Many studies have demonstrated a functional link between Ang II and TGF-β1 in the heart, and both are potent inducers of cardiac hypertrophy. Ang II has been shown to induce the expression of TGF-β1 in cardiac myocytes and fibroblasts (26). The absence of the TGF-β1 gene prevented the development of cardiac hypertrophy in response to subpressor doses of Ang II (27). We have demonstrated previously that genetic or pharmacological blockade of AT1 suppressed cardiac TGF-β1 overexpression and attenuated cardiac hypertrophy in GCA-deficient mice (6, 7). It has also been demonstrated that pharmacological blockade of AT2 is able to attenuate Ang II-stimulated TGF-β1 secretion in valvular interstitial cells (28). In the present study, overexpression of TGF-β1 in GCA deficiency was modulated by deletion of AT2, which also diminished the extent of cardiac hypertrophy. Thus, the present findings suggest that cardiac TGF-β1 participates in GCA-elicited inhibition of AT2-mediated pro-hypertrophic signaling in the heart.

Genetic deletion and pharmacological blockade of AT1 both reversed cardiac hypertrophy in GCA KO mice, thus implicating AT1 in growth promotion (6). Ablation of AT2 in the present study also partially attenuated cardiac hypertrophy in GCA KO mice, but somewhat surprisingly, the AT1 antagonist olmesartan did not produce further decreases in the HW/BW or LVW/BW ratios despite exerting beneficial effects on SBP. Importantly, however, it has been reported that blockade of AT2 abolished the anti-hypertrophic effect of AT1 antagonists in hearts of aged rats (29) and that combined AT1/AT2 blockade did not influence Ang II infusion-dependent cardiac hypertrophy in Sprague Dawley rats (30). The implication of these studies in intact animals, that AT2 is essential for the anti-hypertrophic effects of AT1 antagonists, is supported by the present findings in gene-targeted animals.

The present study further distinguishes the impact of pharmacological AT1 antagonism on SBP from effects on cardiac remodeling. Thus, olmesartan decreased SBP in intact, GCA-null, AT2-null, and GCA/AT2-double null mice, whereas cardiac hypertrophy was reversed by olmesartan only in GCA KO mice. Ang II signaling leading to altered gene transcriptional activation and function may involve multiple intracellular pathways. The AT1 is coupled to heterotrimeric G proteins and may activate phospholipases to increase calmodulin kinase activity and calcium release, which effects vasoconstriction (31). Balanced against this is the activation of ANP and BNP transcription and cross talk with the AT2, which modulate hypertensive actions (31). On the other hand, cardiomyocyte proliferation and hypertrophy are also stimulated by Ang II acting via AT1 signaling through the epidermal growth factor receptor coupled to MAPKs (32, 33). Thus, the present observations that cardiac hypertrophy in GCA deficiency is independent of blood pressure reg-

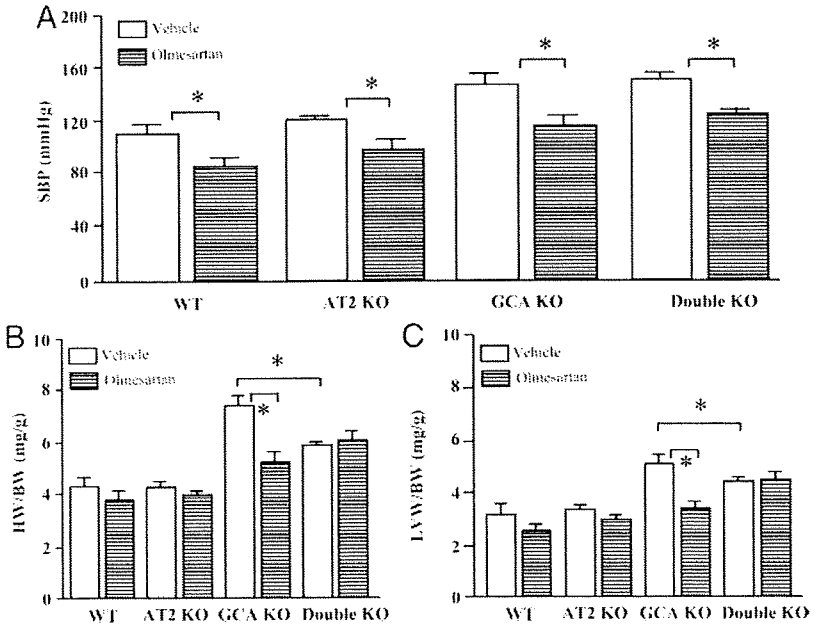

FIG. 6. The AT1 antagonist olmesartan lowered SBP but did not affect cardiac hypertrophic phenotype in double KO mice. A–C, Effect of olmesartan (10 mg/kg orally for 4 wk) on SBP (A), HW/BW (B), and LVW/BW (C) in hearts of mice carrying each of the genotypes under investigation. Values are means ± SEM (n = 7–9). *, $P < 0.05$.

ulation is consistent with the differential activation of alternate signaling cascades by AT1 and AT2.

Recently, several lines of evidence have suggested that GCA activity is relatively decreased in certain populations of patients with cardiovascular diseases. A functional polymorphism in the 5′-flanking region of the human GCA gene that is associated with essential hypertension and cardiac hypertrophy has been described (34). This variant most likely diminishes GCA gene expression in these patients, predisposing them to hypertension and cardiac hypertrophy such as that observed in GCA-deficient mice. Another polymorphism in the human GCA gene 5′-flank modulates left ventricular mass in essential hypertension (35). We also reported that a further polymorphism in the GCA 5′-flanking region, which decreases the transactivation of the GCA promoter in vascular smooth muscle cells, is associated with essential hypertension (36). Furthermore, it is emerging that desensitization of GCA signaling occurs in patients with severe heart failure (37, 38). These lines of evidence suggest that functional deterioration of GCA signaling may contribute to the progression of certain cardiovascular diseases. At this time, it is unclear whether an AT2-dependent mechanism could be operative in these patients. The present findings that cardiac hypertrophy in GCA-null mice is attenuated by blocking AT2 may provide important information for further detailed mechanistic research and eventual application of AT2 antagonists in patients with hypertension and cardiac hypertrophy caused by decreased GCA activity.

Taken together, the present findings demonstrate that GCA inhibits AT2-mediated cardiac growth-promoting signaling pathways and provides new insights into endogenous protective mechanisms against cardiac remodeling.

Acknowledgments

We thank Dr. Akiyoshi Fukamizu (University of Tsukuba, Tsukuba, Ibaraki, Japan) for the AT1a-deficient mice and Dr. David L. Garbers (Howard Hughes Medical Institute and Department of Pharmacology, University of Texas, Southwestern Medical Center at Dallas, Dallas, TX) for GCA-deficient mice.

Address all correspondence and requests for reprints to: Yuhao Li, 54 Kawahara-cho, Shogoin, Sakyo-ku, Kyoto 606-8507, Japan. E-mail: yuhao@kuhp.kyoto-u.ac.jp.

This work was supported in part by research grants from Japanese Ministry of Education, Science and Culture, the Japanese Ministry of Health and Welfare and the Japanese Society for the Promotion of Science.

Disclosure Summary: The authors have nothing to declare.

References

1. Gosse P 2005 Lefr ventricular hypertrophy as a predictor of cardiovascular risk. J Hypertens Suppl 23:S27–S33
2. Nakao K, Itoh H, Saito Y, Mukoyama M, Ogawa Y 1996 The natriuretic peptide family. Curr Opin Nephrol Hypertens 5:4–11
3. Horio T, Nishikimi T, Yoshihara F, Matsuo H, Takishita S, Kangawa K 2000 Inhibitory regulation of hypertrophy by endogenous atrial natriuretic peptide in cultured cardiac myocytes. Hypertension 35:19–24
4. Ogawa Y, Tamura N, Chusho H, Nakao K 2001 Brain natriuretic peptide appears to act locally as an antifibrotic factor in the heart. Can J Physiol Pharmacol 79:723–729
5. Lopez MJ, Wong SK, Kishimoto I, Dubois S, Mach V, Friesen J, Garbers DL, Beuve A 1995 Salt-resistant hypertension in mice lacking the guanylyl cyclase-A receptor for atrial natriuretic peptide. Nature 378:65–68
6. Li Y, Kishimoto I, Saito Y, Harada M, Kuwahara K, Izumi T, Takahashi N, Kawakami R, Tanimoto K, Nakagawa Y, Nakanishi M, Adachi Y, Garbers DL, Fukamizu A, Nakao K 2002 Guanylyl cyclase A inhibits angiotensin II type 1a receptor-mediated cardiac remodeling, an endogenous protective mechanism in the heart. Circulation 106:1722–1728
7. Li Y, Kishimoto I, Saito Y, Harada M, Kuwahara K, Izumi T, Hamanaka I, Takahashi N, Kawakami R, Tanimoto K, Nakagawa Y, Nakanishi M, Adachi Y, Garbers DL, Fukamizu A, Nakao K 2004 Androgen contributes to gender-related cardiac hypertrophy and fibrosis in mice lacking the gene encoding guanylyl cyclase-A. Endocrinology 145:951–958
8. Nakanishi M, Saito Y, Kishimoto I, Harada M, Kuwahara K, Takahashi N, Kawakami R, Nakagawa Y, Tanimoto K, Yasuno S, Usami S, Li Y, Adachi Y, Fukamizu A, Garbers DL, Nakao K 2005 Role of natriuretic peptide receptor GC-A in myocardial infarction evaluated using genetically engineered mice. Hypertension 46:441–447
9. Hunyady L, Turu G 2004 The role of the AT1 angiotensin receptor in cardiac hypertrophy: angiotensin II receptor or stretch sensor? Trends Endocrinol Metab 15:405–408
10. Berry C, Touyz R, Dominiczak AF, Webb RC, Johns DG 2001 Angiotensin receptors: signaling, vascular pathophysiology, and interactions with ceramide. Am J Physiol Heart Circ Physiol 281:H2337–H2365
11. Lopez JJ, Lorell BH, Ingelfinger JR, Weinberg EO, Schunkert H, Diamant D, Tang SS 1994 Distribution and function of cardiac angiotensin AT1- and AT2-receptor subtypes in hypertrophied rat hearts. Am J Physiol 267:H844–H852
12. Suzuki J, Matsubara H, Urakami M, Inada M 1993 Rat angiotensin II (type 1A) receptor mRNA regulation and subtype expression in myocardial growth and hypertrophy. Circ Res 73:439–447
13. Tsutsumi Y, Matsubara H, Ohkubo N, Mori Y, Nozawa Y, Murasawa S, Kijima K, Maruyama K, Masaki H, Moriguchi Y, Shibasaki Y, Kamihata H, Inada M, Iwasaka T 1998 Angiotensin II type 2 receptor is upregulated in human heart with interstitial fibrosis, and cardiac fibroblasts are the major cell type for its expression. Circ Res 83:1035–1046
14. Mifune M, Sasamura H, Shimizu-Hirota R, Miyazaki H, Saruta T 2000 Angiotensin II type 2 receptors stimulate collagen synthesis in cultured vascular smooth muscle cells. Hypertension 36:845–850
15. Senbonmatsu T, Ichihara S Price Jr E, Gaffney FA, Inagami T 2000 Evidence for angiotensin II type 2 receptor-mediated cardiac myocyte enlargement during *in vivo* pressure overload. J Clin Invest 106:R25–R29
16. Ichihara S, Senbonmatsu T, Price Jr E, Ichiki T, Gaffney FA, Inagami T 2001 Angiotensin type 2 receptor is essential for ventricular hypertrophy and cardiac fibrosis in chronic angiotensin II-induced hypertension. Circulation 104:346–351
17. Yan X, Price RL, Nakayama M, Ito K, Schuldt AJ, Manning WJ, Sanbe A, Borg TK, Robbins J, Lorell BH 2003 Ventricular-specific expression of angiotensin II type 2 receptors causes dilated cardiomyopathy and heart failure in transgenic mice. Am J Physiol Heart Circ Physiol 285:H2179–H2187
18. D'Amore A, Black MJ, Thomas WG 2005 The angiotensin II type 2 receptor causes constitutive growth of cardiomyocytes and does not antagonize angiotensin II type 1 receptor-mediated hypertrophy. Hypertension 46:1347–1354
19. Sanada S, Node K, Minamino T, Takashima S, Ogai A, Asanuma H, Ogita H, Liao Y, Asakura M, Kim J, Hori M, Kitakaze M 2003 Long-acting Ca^{2+} blockers prevent myocardial remodeling induced by chronic NO inhibition in rats. Hypertension 41:963–967
20. Lorenzo O, Ruiz-Ortega M, Suzuki Y, Rupérez M, Esteban V, Sugaya T, Egido J 2002 Angiotensin III activates nuclear transcription factor-κB in cultured mesangial cells mainly via AT_2 receptors: studies with AT_1 receptor-knockout mice. J Am Soc Nephrol 13:1162–1171
21. Akishita M, Iwai M, Wu L, Zhang L, Ouchi Y, Dzau VJ, Horiuchi M 2000 Inhibitory effect of angiotensin II type 2 receptor on coronary arterial remodeling after aortic banding in mice. Circulation 102:1684–1689
22. de Bold AJ, Bruneau BG, Kuroski de Bold ML 1996 Mechanical and neuroendocrine regulation of the endocrine heart. Cardiovasc Res 31:7–18
23. Masaki H, Kurihara T, Yamaki A, Inomata N, Nozawa Y, Mori Y, Murasawa S, Kizima K, Maruyama K, Horiuchi M, Dzau VJ, Takahashi H, Iwasaka T, Inada M, Matsubara H 1998 Cardiac-specific overexpression of angiotensin II AT2 receptor causes attenuated response to AT1 receptor-mediated pressor and chronotropic effects. J Clin Invest 101:527–535

24. Inagami T, Senbonmatsu T 2001 Dual effects of angiotensin II type 2 receptor on cardiovascular hypertrophy. Trends Cardiovasc Med 11:324–328
25. Oliviéro P, Chassagne C, Kolar F, Adamy C, Marotte F, Samuel JL, Rappaport L, Ostadal B 2000 Effect of pressure overload on angiotensin receptor expression in the rat heart during early postnatal life. J Mol Cell Cardiol 32:1631–1645
26. Rosenkranz S 2004 TGF-β1 and angiotensin networking in cardiac remodeling. Cardiovasc Res 63:423–432
27. Schultz Jel J, Witt SA, Glascock BJ, Nieman ML, Reiser PJ, Nix SL, Kimball TR, Doetschman T 2002 TGF-β1 mediates the hypertrophic cardiomyocyte growth induced by angiotensin II. J Clin Invest 109:787–796
28. Scott L, Kerr A, Haydock D, Merrilees M 1997 Subendothelial proteoglycan synthesis and transforming growth factor β distribution correlate with susceptibility to atherosclerosis. J Vasc Res 34:365–377
29. Jones ES, Black MJ, Widdop RE 2004 Angiotensin AT2 receptor contributes to cardiovascular remodelling of aged rats during chronic AT1 receptor blockade. J Mol Cell Cardiol 37:1023–1030
30. Brassard P, Amiri F, Schiffrin EL 2005 Combined angiotensin II type 1 and type 2 receptor blockade on vascular remodeling and matrix metalloproteinases in resistance arteries. Hypertension 46:598–606
31. Berry C, Touyz R, Dominiczak AF, Webb RC, Johns DG 2001 Angiotensin receptors: signaling, vascular pathophysiology, and interactions with ceramide. Am J Physiol Heart Circ Physiol 281:H2337–H2365
32. Kim S, Iwao H 2000 Molecular and cellular mechanisms of angiotensin II-mediated cardiovascular and renal diseases. Pharmacol Rev 52:11–34
33. Thomas WG, Brandenburger Y, Autelitano DJ, Pham T, Qian H, Hannan RD 2002 Adenoviral-directed expression of the type 1A angiotensin receptor promotes cardiomyocyte hypertrophy via transactivation of the epidermal growth factor receptor. Circ Res 90:135–142
34. Nakayama T, Soma M, Takahashi Y, Rehemudula D, Kanmatsuse K, Furuya K 2000 Functional deletion mutation of the 5′-flanking region of type A human natriuretic peptide receptor gene and its association with essential hypertension and left ventricular hypertrophy in the Japanese. Circ Res 86:841–845
35. Rubattu S, Bigatti G, Evangelista A, Lanzani C, Stanzione R, Zagato L, Manunta P, Marchitti S, Venturelli V, Bianchi G, Volpe M, Stella P 2006 Association of atrial natriuretic peptide and type A natriuretic peptide receptor gene polymorphisms with left ventricular mass in human essential hypertension. J Am Coll Cardiol 48:499–505
36. Usami S, Kishimoto I, Saito Y, Harada M, Kuwahara K, Nakagawa Y, Nakanishi M, Yasuno S, Kangawa K, Nakao K 2008 Association of CT dinucleotide repeat polymorphism in the 5′-flanking region of the guanylyl cyclase (GC)-A gene with essential hypertension in the Japanese. Hypertens Res 31:89–96
37. Tsutamoto T, Kanamori T, Wada A, Kinoshita M 1992 Uncoupling of atrial natriuretic peptide extraction and cyclic guanosine monophosphate production in the pulmonary circulation in patients with severe heart failure. J Am Coll Cardiol 20:541–546
38. Tsutamoto T, Kanamori T, Morigami N, Sugimoto Y, Yamaoka O, Kinoshita M 1993 Possibility of down-regulation of atrial natriuretic peptide receptor coupled to guanylate cyclase in peripheral vascular beds of patients with chronic severe heart failure. Circulation 87:70–75

Arteriosclerosis, Thrombosis, and Vascular Biology

JOURNAL OF THE AMERICAN HEART ASSOCIATION

American Heart Association®

Learn and Live℠

Human Placental Ectonucleoside Triphosphate Diphosphohydrolase Gene Transfer via Gelatin-Coated Stents Prevents In-Stent Thrombosis

Yasuhiro Takemoto, Hiroyuki Kawata, Tsunenari Soeda, Keiichi Imagawa, Satoshi Somekawa, Yukiji Takeda, Shiro Uemura, Masanori Matsumoto, Yoshihiro Fujimura, Jun-ichiro Jo, Yu Kimura, Yasuhiko Tabata and Yoshihiko Saito

Arterioscler Thromb Vasc Biol 2009;29;857-862; originally published online Mar 26, 2009;

DOI: 10.1161/ATVBAHA.109.186429

Arteriosclerosis, Thrombosis, and Vascular Biology is published by the American Heart Association. 7272 Greenville Avenue, Dallas, TX 72514

 Print ISSN: 1079-5642. Online ISSN: 1524-4636

Human Placental Ectonucleoside Triphosphate Diphosphohydrolase Gene Transfer via Gelatin-Coated Stents Prevents In-Stent Thrombosis

Yasuhiro Takemoto, Hiroyuki Kawata, Tsunenari Soeda, Keiichi Imagawa, Satoshi Somekawa, Yukiji Takeda, Shiro Uemura, Masanori Matsumoto, Yoshihiro Fujimura, Jun-ichiro Jo, Yu Kimura, Yasuhiko Tabata, Yoshihiko Saito

Background—In-stent thrombosis is mainly triggered by adenosine diphosphate (ADP)-dependent platelet aggregation after percutanous coronary stent implantation. Ectonucleoside triphosphate diphosphohydrolase (E-NTPDase) rapidly hydrolyzes ADP to adenosine monophosphate, inhibiting platelet aggregation. We tested the hypothesis that local delivery of human placental E-NTPDase (pE-NTPDase) gene into injured arteries via gene-eluting stent could prevent subacute in-stent thrombosis.

Methods and Results—We generated gene-eluting stents by coating bare metal stents with cationic gelatin hydrogel containing pE-NTPDase cDNA (pE-NTPDase stent), and implanted the stents into rabbit femoral arteries (FA) prone to production of platelet-rich thrombi due to repeated balloon injury at 4-week intervals. After the second injury, E-NTPDase gene expression was severely decreased; however, the implantation of pE-NTPDase stent increased E-NTPDase mRNA levels and NTPDase activity to higher level than normal FA. The FAs with pE-NTPDase stents maintained patency in all rabbits ($P<0.01$), whereas the stent-implanted FAs without pE-NTPDase gene showed low patency rates (17% to 25%). The occlusive platelet-rich thrombi, excessive neointimal growth, and infiltration of macrophages were inhibited in stent implanted FA with pE-NTPDase gene, but not without pE-NTPDase gene.

Conclusions—Human pE-NTPDase gene transfer via cationic gelatin-coated stents inhibited subacute in-stent thrombosis and suppressed neointimal hyperplasia and inflammation without antiplatelet drugs. ***(Arterioscler Thromb Vasc Biol. 2009;29:857-862.)***

Key Words: cationic gelatin ■ E-NTPDase ■ gene therapy ■ thrombosis ■ platelets

In-stent thrombosis is a life-threatening adverse event that often follows coronary stent implantation. The use of polymer-coated drug-eluting stents (DES) has significantly reduced the rates of restenosis and target lesion revascularization (TLR) compared with bare metal stents (BMS). However, such stents do not reduce the incidence of subacute in-stent thrombosis and even increase late in-stent thrombosis attributable to incomplete reendothelialization and vascular healing.[1–3] Therefore, long-term use of antiplatelet drugs is required after DES implantation; this may cause critical adverse events including hemorrhagic complications and thrombotic thrombocytopenic purpura in a small number of cases. Over the past couple of decades, a number of studies have focused on development of new types of coronary stents, such as gene-eluting stents, to prevent restenosis or accelerate reendothelialization[4,5]; however, further efforts to develop stents that prevent in-stent thrombosis without antiplatelet drugs are necessary.

In-stent thrombosis is primarily triggered by local platelet activation, culminating in platelet aggregation, the generation of coagulation factors, and the formation of a fibrin network and a stable occlusive thrombus.[6,7] Plaque rupture or vascular injury resulting from stent implantation or the stent itself can induce initial platelet adhesion and activation. Subsequent intracellular signaling events trigger the release of secondary agonists, such as thromboxane A_2 from membrane phospholipids and adenosine diphosphate (ADP) from dense granules, which led to the production of coagulation factors on the platelet surface and generation of thrombin.[8,9] Finally, subacute in-stent thrombosis occurs. Thus, ADP is a key agonist that triggers platelet aggregation, and degrading ADP or blocking binding of ADP to purinergic receptors on the platelet surface might prevent in-stent thrombosis.[10,11] This concept is clinically supported by evidence that thienopyridines, specific purinergic receptor blockers, significantly prevent subacute thrombosis after coronary artery stent implantation.[12,13]

Received October 9, 2008; revision accepted March 9, 2009.

From the First Department of Internal Medicine (Y.T., H.K., T.S., K.I., S.S., Y.T., S.U., Y.S. and Blood Transfusion Medicine (M.M., Y.F.), Nara Medical University, Japan; and the Department of Biomaterials (U.J., Y.K., Y.T.), Field of Tissue Engineering, Kyoto University, Kyoto, Japan.

Correspondence to Hiroyuki Kawata, MD, First Department of Internal Medicine, Nara Medical University, 840 Shijo-cho, Kashihara, Nara 634-8522, Japan. E-mail hkawata@naramed-u.ac.jp

Arterioscler Thromb Vasc Biol is available at http://atvb.ahajournals.org DOI: 10.1161/ATVBAHA.109.186429

Vascular ectonucleoside triphosphate diphosphohydrolase (vE-NTPDase), or CD39, is a membrane-bound enzyme that plays a crucial role in vascular endothelial function by inhibiting platelet aggregation via phosphohydrolysis of ATP and ADP to AMP.[14] vE-NTPDase has 2 putative transmembrane domains and an extracellular domain containing 5 apyrase conserved regions (ACRs), of which ACR-1, -4, and -5 are important for enzymatic activity.[15] Makita et al[16] purified human placental E-NTPDase (pE-NTPDase), an alternative form of vE-NTPDase that differs at the N-terminal 11-aa residues. The purified pE-NTPDase has been demonstrated to have 2 putative transmembrane domains and an extracellular domain containing an enzymatically active region like vE-NTPDase. This protein also inhibits platelet aggregation induced by platelet agonists or shear stress.[16,17] Recently, Furukoji et al[18] reported that human pE-NTPDase gene transfer to air-injured arteries via adenovirus vector suppressed platelet aggregation, thrombus formation, and neointimal growth in mice. Based on these findings, we speculate that local delivery of the pE-NTPDase gene through a gene-eluting stent might prevent subacute in-stent thrombosis and neointimal hyperplasia without requiring antiplatelet agents.

To evaluate antithrombotic effects of the gene-eluting stent in a clinic-like setting, we used a repeated balloon injury model in the rabbit femoral artery, which is similar to acute coronary syndrome (ACS) in pathogenesis of occlusive thrombi.[19,20] In this study, we generated a new coronary stent coated with biodegradable cationic gelatin hydrogel as a platform for gene elution and evaluated the effects of human pE-NTPDase gene transfer to injured arteries on prevention of subacute in-stent thrombosis and smooth muscle cell proliferation using the rabbit ACS-like thrombus model.

Methods

Please see the supplemental materials at http://atvb.ahajournals.org for detailed Methods.

Platelet Aggregation

We evaluated the effects of human pE-NTPDase on rabbit platelet aggregation induced by ADP as previously described.[16,18]

Preparation of Cationic Gelatin-Coated Stents

Cationic gelatin hydrogel was generated as previously described.[21] Normal stainless steel stents (bare metal stents [BMS]) were coated with cationic gelatin hydrogels to prepare the gene-eluting stents.

Plasmid Expression Vectors and Gene-Eluting Stents

The human pE-NTPDase cDNA was FLAG-tagged at the N terminus in the pBS CAG vector.[17] We also constructed a control pBS CAG vector encoding bacterial β-galactosidase (LacZ) to evaluate effective transduction of plasmid DNA from a stent platform into rabbit arterial tissue. We generated pE-NTPDase gene-eluting stent (pE-NTPDase stent) and LacZ gene-eluting stent (LacZ stent) with the use of the stent coated with cationic gelatin hydrogel (gelatin-coated stent).

Repeated-Balloon Injury of Rabbit Femoral Arteries

The Animal Experimentation Committee at Nara Medical University approved the experimental protocol used in this study. We used 76 male Japanese white rabbits (SLC Japan, Shizuoka, Japan) weighing 2.5 to 2.7 kg. Repeated-balloon injury of the right femoral artery (FA) was performed to induce platelet-rich thrombus similar to ACS as previously described, with minor modification.[19,20]

In Vivo Stent Implantation

Rabbits were assigned to 1 of 4 groups: 22 rabbits received BMS, 22 gelatin-coated stents, 10 LacZ stents, and 22 pE-NTPDase stents. Each stent was implanted in the injured right FA by balloon inflation.

Evaluation of Patency of Stent Implanted Arteries

Transcutaneous continuous Doppler analysis on day 3 post stent implantation (n=10 for the BMS, gelatin-coated stent, and pE-NTPDase stent groups, and n=4 for the LacZ stent group), and angiography on days 3 and 7 post stent implantation (n=10 and 12 on each day for the BMS, gelatin-coated stent, and pE-NTPDase stent groups, n=4 and 6 on each day for the LacZ stent group) were carried out to evaluate the patency of the stent implanted arteries.

X-Gal Staining, PCR, Western Blotting, and Immunohistochemistry

X-Gal staining of stent implanted FAs, evaluation of E-NTPDase and endothelial nitric oxide synthase (eNOS) mRNA expression by real-time polymerase chain reaction (PCR) and E-NTPDase protein expression by Western blotting in stent implanted FAs, and immunohistochemical examination were performed as previously described (please see the supplemental Methods).

Measurement of NTPDase Activity

NTPDase activity of whole FAs of stent implanted site was measured by luciferin-luciferase bioluminescence assay using an ATP assay system (TOYO B-Net CO, LTD) on days 3 and 7 post stent implantation (n=3 and 4 on each day, respectively, for the BMS and pE-NTPDase stent groups). The data were expressed as the ratio of activity in stent implanted FAs to activity in contralateral normal FA.

Statistical Analysis

Data are expressed as means±SD. Differences between individual groups were evaluated using the unpaired Student *t* test or ANOVA with Bonferroni multiple comparisons. Values of $P<0.05$ were considered significant.

Results

Effects of Human Placental E-NTPDase on Rabbit Platelet Aggregation

First, we investigated whether platelet aggregation was induced by ADP in rabbits, as well as the effects of human pE-NTPDase on rabbit platelet aggregation. Rabbit platelet aggregation was induced by ADP, and this was significantly suppressed by human pE-NTPDase (supplemental Figure I), indicating that human pE-NTPDase might inhibit ADP-dependent platelet aggregation also in rabbits.

Successful Gene Transfer via Gelatin-Coated Stent in Vivo

To evaluate gene transfer and protein expression in the injured arterial tissue, we implanted LacZ stents into rabbit FAs after repeated-balloon injury, and performed X-Gal staining on days 3 and 7 post implantation in the BMS, gelatin-coated stent, and LacZ stent groups (n=3 on each day). In the LacZ stent group, strong X-Gal staining was observed in the implanted FA on days 3 and 7 (supplemental Figure II), whereas no staining was observed in the arteries of the BMS or gelatin-coated stent groups on day 3 (supplemental Figure II) or 7 (data not shown).

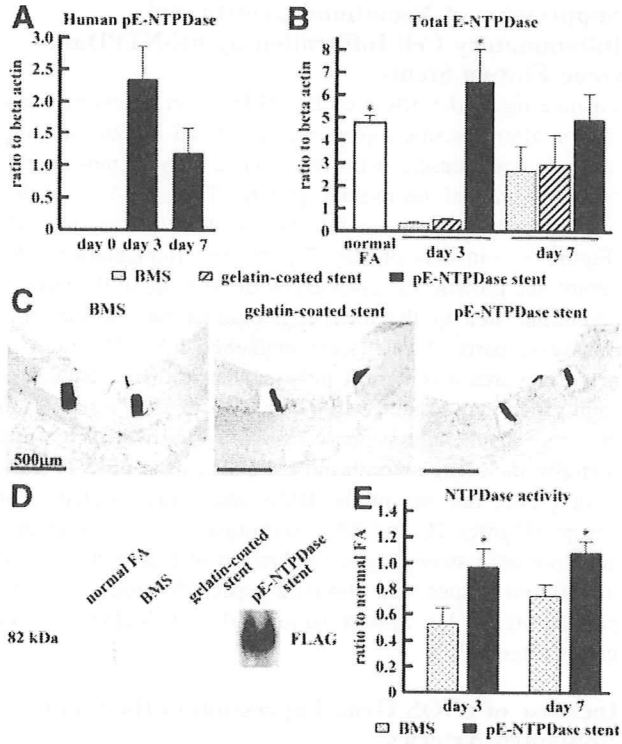

Figure 1. Expression of human pE-NTPDase mRNA (A) and total E-NTPDase mRNA (B) in the stent implanted FAs (*$P<0.01$ vs the BMS and gelatin-coated stent groups on day 3). Expression of human pE-NTPDase protein was examined by immunohistochemical examination (C) and by Western blotting with antibody against FLAG (D). NTPDase activity was measured by luciferin-luciferase bioluminescence assay (E) (*$P<0.05$ vs the BMS group).

These data suggest successful and continuous protein expression after gene transfer from cationic gelatin-coated stents.

E-NTPDase Gene Expression in Stent Implanted Arteries

We examined the expression of E-NTPDase mRNA in the FAs on days 3 and 7 post implantation by real-time PCR and expressed the data as the ratio of E-NTPDase mRNA to β-actin mRNA. As shown in Figure 1A, human pE-NTPDase mRNA expression in the FA was observed 3 days after pE-NTPDase stent implantation and persisted until 7 days after implantation; human pE-NTPDase mRNA was not detected immediately after stent implantation (day 0). In contrast, human pE-NTPDase expression was not observed at any time point in either the BMS or gelatin-coated stent group. We also examined total E-NTPDase mRNA expression of both exogenous human pE-NTPDase and endogenous rabbit vE-NTPDase by real-time PCR (Figure 1B). In the BMS and gelatin-coated stent groups, after the second balloon injury the total E-NTPDase mRNA level was reduced to about 10% of that in normal vessels on day 3 and then recovered to 50% to 60% of normal levels on day 7. However, in the pE-NTPDase stent group, total mRNA levels of E-NTPDase increased by 40% on day 3 and decreased slightly to levels comparable to normal at day 7. These results indicate that human pE-NTPDase gene transfer allowed maintenance of total E-NTPDase mRNA levels in injured vessel walls despite denudation of endothelial cells.

Table. Patency of Stent Implanted FAs

	BMS n (%)	Gelatin-Coated Stent n (%)	LacZ Stent n (%)	pE-NTPDase Stent n (%)
Color Doppler study (day 3)				
Patent	1/10 (10)	1/10 (10)	0/4 (0)	10/10 (100)*
Stenosis	5/10 (40)	6/10 (60)	3/4 (75)	0/10 (0)
Occlusion	4/10 (40)	3/10 (30)	1/4 (25)	0/10 (0)
Angiographical patency				
Day 3	5/10 (50)	5/10 (50)	2/4 (50)	10/10 (100)†‡
Day 7	3/12 (25)	3/12 (25)	1/6 (17)	12/12 (100)*

*$P<0.01$ vs the other groups; †$P<0.01$ vs BMS and gelatin-coated stent group; ‡$P<0.05$ vs the other groups.

E-NTPDase Protein Expression and Enzymatic Activity

Immunostaining for human pE-NTPDase (YH34) revealed that human pE-NTPDase was expressed mainly in smooth muscle cells widely from the media to the surface of neointima but not in the adventitial cells only in the pE-NTPDase stent implanted FAs, though was not detected in the other stent implanted FAs either on day 3 (data not shown) or 7 (Figure 1C). We evaluated pE-NTPDase protein expression in FAs by Western blotting using anti-FLAG antibody, because YH34 did not work in Western blotting. As expected, FLAG was detected only in the pE-NTPDase stent group, and not in the BMS or gelatin-coated stent groups or in normal arteries on day 3 (data not shown) or 7 (Figure 1D) post implantation. Consistent with the E-NTPDase gene and protein expression, NTPDase activity in FAs implanted with the pE-NTPDase stents was similar to that in contralateral normal FAs, and was significantly higher than in FAs implanted with BMS on both days 3 and 7 ($P<0.05$, Figure 1E).

Patency of Stent Implanted Arteries

We evaluated blood flow in the stent implanted FAs by transcutaneous continuous Doppler on day 3 and angiography on days 3 and 7 post implantation. Peak flow velocity measured by continuous Doppler on day 3 showed normal blood flow and patency in all of the arteries implanted with pE-NTPDase stents (10 of 10), whereas normal flow was observed in only 1 of 10 arteries in each of the BMS and gelatin-coated stent groups. Normal flow was not observed in any artery in the LacZ stent group (0 of 4; Table). The rate of angiographic patency in stent implanted FAs in the pE-NTPDase group was significantly higher than in the other 3 groups on both day 3 (100% in the pE-NTPDase stent group versus 50% in the other groups) and day 7 (100% in the pE-NTPDase stent group versus 25% in the BMS and gelatin-coated stent groups, 17% in the LacZ stent group; Table). Representative Doppler flow patterns are shown in supplemental Figure III, and representative angiography are in Figure 2A and supplemental movies. The difference in patency rate between continuous Doppler and angiographic data in the BMS, gelatin-coated stent, and LacZ stent groups might be attributable to collateral flow to the distal site from

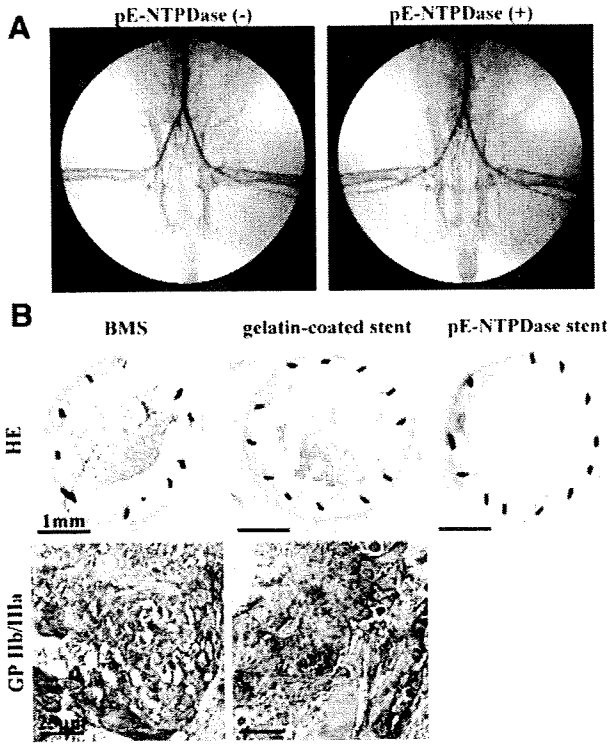

Figure 2. A, Representative angiograms taken on day 7. Arrows and arrowheads show the proximal and distal stent edges, respectively. B, Representative microphotographs of stent implanted FAs on day 7. Thrombi obtained from BMS (lower left) or gelatin-coated stent (lower right) implanted FAs were strongly immunopositive for GP IIb/IIIa.

the proximal site of stent implantation affecting the continuous Doppler measurement.

Inhibition of In-Stent Thrombosis by pE-NTPDase Gene Eluting Stents

As shown in Figure 2B, histological examination demonstrated occlusive in-stent thrombosis in the BMS or gelatin-coated stent implanted FAs, whereas no thrombi were observed in FAs implanted with E-NTPDase stents on day 7 post implantation. Additionally, immunostaining for GP IIb/IIIa showed that the occlusive thrombi in the BMS and gelatin-coated stent groups contained a large amount of platelets. These results suggest that human pE-NTPDase gene eluting stent suppressed platelet aggregation in the injured arteries, inhibiting subacute in-stent thrombosis without antiplatelet drugs.

Suppression of Neointimal Growth and Inflammatory Cell Infiltration by pE-NTPDase Gene Eluting Stents

To investigate the effect of E-NTPDase on neointimal formation after vascular injury, we performed immunostaining for α-smooth muscle actin to evaluate smooth muscle cell proliferation and neointimal growth (Figure 3A), and for macrophages to evaluate infiltration of inflammatory cells (Figure 3C) in FAs on day 7 post stent implantation. The neointimal growth was assessed by the average of the ratio of neointima area to the area of neointima plus media in 3 transverse parts of each stent implanted FAs. The ratio of neointima area was significantly smaller in the pE-NTPDase stent group than in the BMS group (Figure 3B; $P<0.05$). On the other hand, stent struts were all covered with neointima partially including smooth muscle cells in the pE-NTPDase stent group, but not in the BMS and gelatin-coated stent groups (Figures 2B and 3A). Additionally, in the BMS and gelatin-coated stent groups, infiltration of macrophages into the arterial tissues was observed especially around the implanted stents, but almost none in the pE-NTPDase stent group (Figure 3C).

Increase of eNOS Gene Expression in the Stent Implanted Arteries

We evaluated the eNOS mRNA expression in the neointima of stent-implanted FAs to speculate the reendothelialization after stent implantation, because several antibodies that recognize markers of endothelial cells, such as CD31, von willebrand factor, or eNOS, did not work for immunostaining in plastic resin-embedded samples. The levels of eNOS mRNA expression in the neointima of FAs in the pE-NTPDase stent group were higher than in the BMS and gelatin-coated stent groups on both day 3 and 7, and recovered to 80% of normal level on day 7 (Figure 4). In the BMS and gelatin-coated stent group, the levels of eNOS mRNA expression were extremely low on day 3 and recovered to 40% to 50% of normal level on day 7. These results indicate that reendothelialization is accelerated in the pE-NTPDase stent implanted arteries, and that the recovery of the E-NTPDase mRNA expression on day 7 in the BMS and gelatin-coated stent groups (Figure 1B) is caused partly by the newly regenerated endothelial cells.

Discussion

This study is the first to report that: (1) a plasmid vector encoding the pE-NTPDase gene is reliably incorporated into

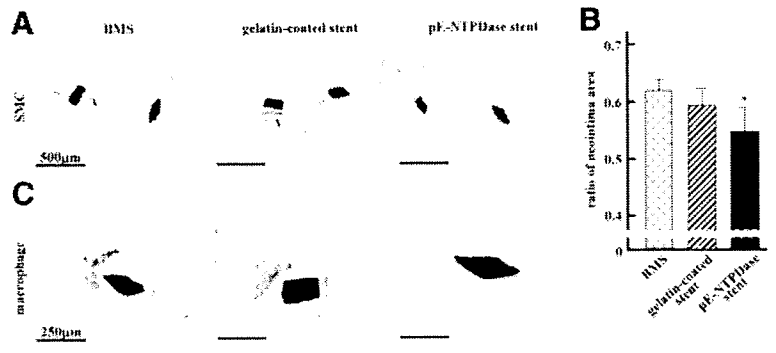

Figure 3. A, Immunohistochemical staining for α-smooth muscle actin in the stent implanted FAs. B, The graph showing the ratio of neointima area calculated by the ratio of neointima area to the area of neointima plus media ($^*P<0.05$ vs the BMS group). C, Immunohistochemical staining for macrophage in the stent implanted FAs.

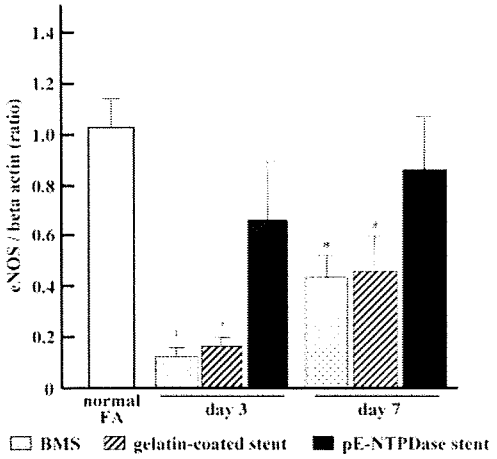

Figure 4. eNOS mRNA expression in the neointima of the stent implanted FAs. Data are expressed as the ratio of eNOS mRNA to β-actin mRNA (*$P<0.05$ and †$P<0.01$ vs normal FA).

and released from newly designed cationic gelatin-coated stents, (2) local delivery of the pE-NTPDase gene into injured arteries enhances the mRNA and protein expression of pE-NTPDase, thereby (3) preventing subacute in-stent thrombosis in a rabbit model of ACS-like thrombus formation without antiplatelet therapy, and (4) the locally enhanced expression of pE-NTPDase may suppress neointimal hyperplasia and inflammation, and accelerate reendothelialization in arteries after stent implantation.

E-NTPDase, which is primarily expressed in the endothelial cells of normal vessels, rapidly hydrolyzes extracellular ATP and ADP to AMP, which is further converted to the antithrombotic and antiinflammatory mediator adenosine by 5′-nucleotidase. Thus, E-NTPDase plays a critical role in the inhibition of platelet aggregation in the vasculature. However, in injured vessels, E-NTPDase activity decreases, causing accumulation of ADP and thrombus formation. In fact, in the present study, vE-NTPDase mRNA levels were decreased to about one tenth of that in normal vessels (Figure 1B) after repetitive injury. The E-NTPDase mRNA levels in the FAs implanted with BMS or gelatin-coated stent recovered to 50% to 60% of normal levels on day 7 though without human pE-NTPDase gene transfer. On the other hand, the mRNA expression of eNOS, which is specifically expressed in endothelial cells, was recovered to about 45% of normal level on day 7 in the BMS or gelatin-coated stent implanted FAs (Figure 4). Therefore, in the stent implanted arteries without human pE-NTPDase gene, the recovery of E-NTPDase mRNA levels was comparatively parallel with that of eNOS mRNA levels. Based on these data, we speculate that the recovery of E-NTPDase gene expression on day 7 in the BMS or gelatin-coated stent implanted FAs was partly induced by the newly regenerated endothelial cells.

On the other hand, as shown in Figure 1B, human pE-NTPDase gene transfer augmented the total levels of E-NTPDase mRNA to levels similar to or higher than those observed in normal vessels throughout the 7-day experimental period, resulting in inhibition of in-stent thrombosis. Several previous observations[22,23] showed that overexpression of the E-NTPDase gene by adenoviral transfection or genetic engineering methods could result in resistance to thrombosis, supposing that high expression level of E-NTPDase is necessary to block thrombosis. However, the present study suggests that keeping the physiological levels of E-NTPDase is enough to prevent in-stent thrombosis after stenting. Immunohistochmical examination showed pE-NTPDase protein was mainly expressed in smooth muscle cells from media to the surface of neointima, suggesting pE-NTPDase expressed in the surface of the injured vessel prevents platelet aggregation.

The data of early recovery of eNOS mRNA expression in neointima in the pE-NTPDase stent implanted FAs indicates the acceleration of reendothelialization by the human pE-NTPDase gene transfer, which may play a part in preserving total E-NTPDase gene expression in the pE-NTPDase stent implanted arteries in subacute phase. Additionally, immunohistochemical examination (Figure 3) demonstrated that neointimal hyperplasia attributable to smooth muscle cell proliferation and macrophage infiltration after stent implantation was inhibited by the pE-NTPDase gene-eluting stent. Therefore, the pE-NTPDase gene-eluting stent prevents in-stent thrombosis in subacute phase, and may be able to prevent restenosis and late thrombosis by both acceleration of reendothelialization and suppression of neointimal hyperplasia and inflammation. Several recent studies[18,24,25] have indicated effects of E-NTPDase beyond the regulation of platelet aggregation, which support the data of our present study. A mouse model showed that gene transfer of human E-NTPDase into injured arteries inhibited smooth muscle cell proliferation.[18] In a mouse model of angiogenesis induced by VEGF and fibroblast growth factor, E-NTPDase knockout resulted in the failure of migration and recruitment of monocytes and endothelial cells to the angiogenic site and consequently impaired angiogenesis.[24] Mizumoto et al also reported that inflammatory response was exacerbated in E-NTPDase knockout mice.[25]

To date, no stent has been developed that focuses on prevention of in-stent thrombosis, although first-generation drug-eluting stents developed to reduce restenosis are in widespread clinical use. In addition, a number of new types of stent that accelerate reendothelialilzation are under development. Considering that in-stent thrombosis remains a major cause of death and morbidity after percutaneous coronary intervention, future stents should be developed to have antithrombotic as well as antirestenosis functions. In this context, E-NTPDase represents a promising target for drug development.

Stents are an ideal platform for localized delivery of drugs or genes to the vascular wall. For this purpose, stainless balloon-expandable stents coated with nonerodable polymers or phosphorylcholine, containing drugs or plasmids were developed.[4,5] First generation drug-eluting stents, which use nonerodable polymers reservoirs, have recently been reported to provoke arterial hypersensitivity reactions, such as eosinophilic infiltration and in-stent thrombosis, in a small number of cases.[1,2,26] Instead of nonerodable polymers or phosphorylcholine, we adopted cationic gelatin hydrogel to generate the gene-eluting stents used in the present study. Gelatin is biodegradable and has been proven to be biologically innocuous, it has been widely used for medical and pharmaceutical

applications, and its biosafety has been proven through long clinical use as a surgical biomaterial. In addition, we have recently succeeded in controlling the gradual release of plasmid DNA from cationic gelatin hydrogel in vivo.[21] In this study, successful gene transfer was demonstrated by the expression of human pE-NTPDase and control β-galactosidase in stent-implanted arteries for 7 days after implantation. Histological examination revealed that infiltration of macrophages was not observed in the pE-NTPDase stent implanted FAs (Figure 3C), and was not accelerated by gelatin-coated stents compared to BMS, although the follow-up period is probably not sufficiently long to draw conclusions. Furthermore, based on angiographic data showing no difference in occlusion rate between BMS and gelatin-coated groups, gelatin itself does not seem to accelerate platelet activation or thrombus formation. Therefore, cationic gelatin-coated stents may eventually prove to be safe and useful for gene transfer after coronary intervention.

Indeed the pE-NTPDase protein-eluting stents may be expected to be more effective than gene-eluting stents in point of early exertion of antithrombotic effect in early phase after stent implantation, but we had not generated the adequate gelatin for protein release in vivo. So, we tested the effects of the pE-NTPDase gene-eluting stents in this study. Further investigations are needed to demonstrate the effects of the pE-NTPDase protein-eluting stents.

In summary, human pE-NTPDase gene transfer via cationic gelatin-coated stents prevented subacute in-stent thrombosis by preserving local NTPDase activity, suppressed neointimal hyperplasia and inflammation, and might accelerate reendothelialization. These findings provide a starting point to develop next generation stents that are not susceptible to in-stent thrombosis.

Sources of Funding

This study was supported by a grant-in-aid from the Ministry of Education, Science, and Culture of Japan (No. 19790538) to Dr Kawata.

Disclosures

None.

References

1. Virmani R, Guagliumi G, Farb A, Musumeci G, Grieco N, Motta T, Mihalcsik L, Tespili M, Valsecchi O, Kolodgie FD. Localized hypersensitivity and late coronary thrombosis secondary to a sirolimus-eluting stent: should we be cautious? *Circulation*. 2004;109:701–705.
2. Joner M, Finn AV, Farb A, Mont EK, Kolodgie FD, Ladich E, Kutys R, Skorija K, Gold HK, Virmani R. Pathology of drug-eluting stents in humans. Delayed healing and late thrombotic risk. *J Am Coll Cardiol*. 2006;48:193–202.
3. Moses JW, Leon MB, Popma JJ, Fitzgerald PJ, Holmes DR, O'Shaughnessy C, Caputo RP, Kereiakes DJ, Williams DO, Teirstein PS, Jaeger JL, Kuntz RE, for the SIRIUS Investigators. Sirolimus-eluting stents versus standard stents in patients with stenosis in a native coronary artery. *N Engl J Med*. 2003;349:1315–1323.
4. Johnson TW, Wu YX, Herdeg C, Baumbach A, Newby AC, Karsch KR, Oberhoff M. Stent-based delivery of tissue inhibitor of metalloproteinase-3 adenovirus inhibits neointimal formation in porcine coronary arteries. *Arterioscler Thromb Vasc Biol*. 2005;25:754–759.
5. Egashira K, Nakano K, Ohtani K, Funakoshi K, Zhao G, Ihara Y, Koga J, Kimura S, Tominaga R, Sunagawa K. Local delivery of anti-monocyte chemoattractant protein-1 by gene-eluting stents attenuates in-stent stenosis in rabbits and monkeys. *Arterioscler Thromb Vasc Biol*. 2007;27:2563–2568.
6. Farb A, Sangiorgi G, Carter AJ, Walley VM, Edwards WD, Schwartz RS, Virmani R. Pathology of acute and chronic coronary stenting in humans. *Circulation*. 1999;99:44–52.
7. Gawaz M. Role of platelets in coronary thrombosis and reperfusion of ischemic myocardium. *Cardiovasc Res*. 2004;61:498–511.
8. Gordon EL, Pearson JD, Slakey LL. The hydrolysis of extracellular adenosine nucleotides by cultured endothelial cells from pig aorta. *J Biol Chem*. 1986;261:15496–15504.
9. Pearson JD, Gordon JL. Vascular endothelial and smooth muscle cells in culture selectively release adenine nucleotides. *Nature*. 1979;281:384–386.
10. Zimmermann H. 5'-Nucleotidase: molecular structure and functional aspects. *Biochem J*. 1992;285:345–365.
11. Gachet C. ADP receptors of platelets and their inhibition. *Thromb Haemost*. 2001;6:222–232.
12. Leopold JA, Antman EM. Dual antiplatelet therapy for coronary stenting: a clear path for a research agenda. *Circulation*. 2005;111:1097–1099.
13. Gurbel PA, Bliden KP, Samara W, Yoho JA, Hayes K, Fissha MZ, Tantry US. Clopidogrel effect on platelet reactivity in patients with stent thrombosis. Results of the CREST study. *J Am Coll Cardiol*. 2005;46:1827–1832.
14. Marcus AJ, Johan Broekman M, Drosopoulos JH, Islam N, Alyonycheva TN, Safier LB, Hajjar KA, Posnett DN, Schoenborn MA, Schooley KA, Gayle RB, Maliszewski CR. The endothelial cell ecto-ADPase responsible for inhibition of platelet function is CD39. *J Clin Invest*. 1997;99:1351–1360.
15. Schulte am Esch JII, Sévigny J, Kaczmarek E, Siegel JB, Imai M, Koziak K, Beaudoin AR, Robson SC. Structural elements and limited proteolysis of CD39 influence ATP diphosphohydrolase activity. *Biochemistry*. 1999;38:2248–2258.
16. Makita K, Shimoyama T, Sakurai Y, Yagi H, Matsumoto M, Narita N, Sakamoto Y, Saito S, Ikeda Y, Suzuki M, Titani K, Fujimura Y. Placental ecto-ATP diphosphohydrolase: its structural feature distinct from CD39. localization and inhibition on shear-induced platelet aggregation. *Int J Hematol*. 1998;68:297–310.
17. Matsumoto M, Sakurai Y, Kokubo T, Yagi H, Makita K, Matsui T, Titani K, Fujimura Y, Narita N. The cDNA cloning of human placental ecto-ATP diphosphohydrolases I and II. *FEBS Lett*. 1999;453:335–340.
18. Furukoji E, Matsumoto M, Yamashita A, Yagi H, Sakurai Y, Marutsuka K, Hatakeyama K, Morishita K, Fujimura Y, Tamura S, Asada Y. Adenovirus-mediated transfer of human placental ectonucleoside triphosphate diphosphohydrolase to vascular smooth muscle cells suppresses platelet aggregation in vitro and arterial thrombus formation in vivo. *Circulation*. 2005;111:808–815.
19. Yamashita A, Furukoji E, Marutsuka K, Hatakeyama K, Yamamoto H, Tamura S, Ikeda Y, Sumiyoshi A, Asada Y. Increased vascular wall thrombogenicity combined with reduced blood flow promotes occlusive thrombus formation in rabbit femoral artery. *Arterioscler Thromb Vasc Biol*. 2004;24:2420–2424.
20. Kawata H, Naya N, Takemoto Y, Uemura S, Nakajima T, Horii M, Takeda Y, Fujimoto S, Yamashita A, Asada Y, Saito Y. Ultrasound accelerates thrombolysis of acutely induced platelet-rich thrombi similar to those in acute myocardial infarction. *Circ J*. 2007;71:1643–1648.
21. Kushibiki T, Tomoshige R, Fukunaka Y, Kakemi M, Tabata Y. In vivo release and gene expression of plasmid DNA by hydrogels of gelatin with different cationization extents. *J Control Release*. 2003;90:207–216.
22. Imai M, Takigami K, Guckelberger O, Kaczmarek E, Csizmadia E, Bach FH, Robson SC. Recombinant adenoviral mediated CD39 gene transfer prolongs cardiac xenograft survival. *Transplantation*. 2000;70:864–870.
23. Dwyer KM, Robson SC, Nandurkar HH, Campbell DJ, Gock H, Murray-Segal LJ, Fisicaro N, Mysore TB, Kaczmarek E, Cowan PJ, d'Apice AJ. Thromboregulatory manifestations in human CD39 transgenic mice and the implications for thrombotic disease and transplantation. *J Clin Invest*. 2004;113:1440–1446.
24. Goepfert C, Sundberg C, Sévigny J, Enjyoji K, Hoshi T, Csizmadia E, Robson S. Disordered cellular migration and angiogenesis in cd39-null mice. *Circulation*. 2001;104:3109–3115.
25. Mizumoto N, Kumamoto T, Robson SC, Sevigny J, Matsue H, Enjyoji K, Takashima A. CD39 is the dominant Langerhans cell-associated ecto-NTPDase: modulatory roles in inflammation and immune responsiveness. *Nature Med*. 2002;8:358–365.
26. Lüscher TF, Steffel J, Eberli FR, Joner M, Nakazawa G, Tanner FC, Virmani R. Drug-eluting stent and coronary thrombosis: biological mechanisms and clinical implications. *Circulation*. 2007;115:1051–1058.

Supplement Material

Methods

Effects of Human pE-NTPDase on rabbit platelet aggregation

We had previously purified human pE-NTPDase glycoprotein[1], and in this study we evaluated the effects of human pE-NTPDase on rabbit platelet aggregation induced by ADP as previously described.[1,2] Rabbit platelet-rich plasma (3×10^8 platelets/ml) was incubated in siliconized cuvettes at 37°C for 5 minutes with or without purified human pE-NTPDase (1.5 μg/ml, final concentration). ADP (1 μg/ml, final concentration) was then added to the cuvettes and platelet aggregation was measured with the use of NKK Hematracer-1 (SSR Engineering, Tokyo).

Cationization of Gelatin and Preparation of Cationic Gelatin-Coated Stens

Ethylenediamine and 1-ethyl-3-(3-dimethylaminopropyl) carbodiimide hydrochloride salt were added to 250 ml of 100 mM phosphate-buffered solution (pH 5.0) containing 5 g of gelatin. After dialysis, the solution was freeze-dried to obtain cationic gelatin hydrogel. The cationic ratio was determined by the conventional trinitrobenzene sulfonate (TNBS) method.[3,4] Normal stainless steel stents (bare metal stents, BMS) were incubated in aqueous solutions of 10% cationic gelatin for 5 minutes, and left at 4°C overnight. The cationic gelatin hydrogel was cross-linked to the stents in HCl-acetone (3:7, v/v) containing 0.31 mg/ml glutaraldehyde at 4°C for 24 hours. The stents were immersed in 100 mM glycine solution at 4°C for 24 hours to remove residual aldehyde. Stents were rinsed three times with double distilled water and freeze-dried. The successful coating of stents with cationic gelatin hydrogel was confirmed by coomassie brilliant blue staining.

Preparation of Gene-Eluting Stents

Gelatin-coated stents were incubated in plasmid DNA solutions (pE-NTPDase or Lac Z (1 mg/ml)) so that they would absorb the plasmid. Five gelatin-coated stents were steeped in ^{125}I-labeled plasmid DNA solution (1 mg/ml) to measure the amount of plasmid DNA absorbed. After drying, the radioactivity was measured with a gamma counter (ARC-301B, Aloka). The mean amount of plasmid DNA content in five gelatin-coated stents calculated by radioactivity was 78.3 ± 5.1 μg, which suggests that each gene eluting stent accommodated almost same amount of plasmid DNA.

Repeated-Balloon Injury of Rabbit Femoral Arteries

On two occasions separated by a 4-week interval, the rabbits were anesthetized with pentobarbital sodium (25 mg/kg body weight, i.v.) and subjected to balloon injury of the right femoral artery (FA). Briefly, the first injury was induced by fluoroscopically inserting a Fogarty 2F balloon catheter (Edwards Lifesciences, CA, USA) via the right anterior tibial artery into the right femoral artery, where it was inflated to 1.5 atm. The inflated balloon was then pulled back a distance of 1.0 cm three times. Four weeks later, formation of a stenotic lesion at the site of injury was confirmed angiographically, and then the second injury was induced. In this case, a PTCA balloon catheter (2.75 mm-diameter, 15 mm-length) was inserted via the introducer sheath in the right carotid artery to a site just distal to the stenotic lesion, and a second injury was induced in the same manner as the first. After the second injury, platelet-rich thrombus formation similar to ACS was induced.

In Vivo Stent Implantation

Angiography of rabbit FAs was performed 5 minutes after the second injury to confirm that no occlusion of the injured site or flow delay indicating distal occlusion occurred. Immediately following, 500 U of heparin was administered via a sheath in